Fully depleted, back-illuminated CCDs for astronomy and astrophysics

Steve Holland

Lawrence Berkeley National Laboratory

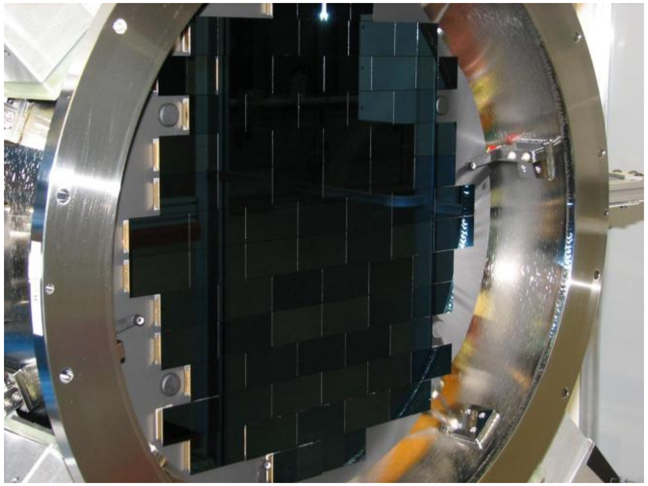

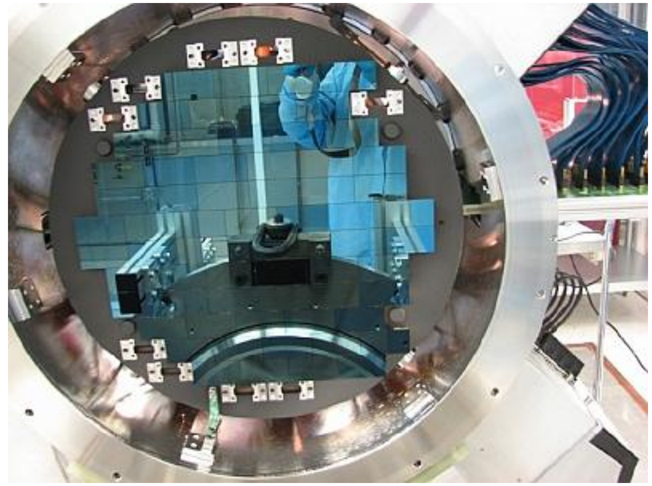

Fermi National Accelerator Laboratory
Dark Energy Survey Camera (DECam)

570 Mpixel camera consisting of 74,
250 μm thick, fully depleted CCDs
Teledyne DALSA/LBNL
1st light Fall 2012

Outline

- Fundamentals of CCDs and CMOS image sensors
- Scientific CCDs for astronomy
- Fully depleted CCDs fabricated on high-resistivity silicon – device physics/applications/technology

Scientific CCDs vs cell phone imager

Unofficial comparison, scientific CCD versus CMOS image sensor for cell phones (e.g. iPhone 4, TSMC/OmniVision[1])

Parameter	CMOS cell phone	Scientific CCD
# pixels	5 - 8 Megapixels	8 – 16 Megapixels
Pixel size	1.4 – 1.7 μm	10 – 15 μm
Imaging area	15 mm^2 (5M)	3775 mm^2 (16M)
Technology	130 nm CMOS	2.5 μm CCD
Illumination	Back illumination	Back illumination
Optical thickness	~ 3 μm	10 – 250 μm
Peak QE	~ 55% (color filter)	~ 90 – 95%
Operating temp	Up to 50°C	-100°C – -140°C
Dark current	20 – 30 e-/pixel/sec	Few e-/pixel/hr
Read noise	~ 2 e-	~ 2-5 e-
Full well	~ 4500 e-	~ 200,000 e- (15 μm)

[1]Rhodes, 2009 IISW Symp. On Backside Illumination of Solid-State Image Sensors, imagesensors.org and http://image-sensors-world.blogspot.com/2010/06/iphone-4-bsi-sensor-is-omnivisions.html

Scientific CCDs vs cell phone imager

Unofficial comparison, scientific CCD versus CMOS image sensor for cell phones (e.g. iPhone 4, TSMC/OmniVision[1])

Parameter	CMOS cell phone	Scientific CCD
# pixels	5 - 8 Megapixels	8 – 16 Megapixels
Pixel size	1.4 – 1.7 µm	10 – 15 µm
Imaging area	15 mm^2 (5M)	3775 mm^2 (16M)
Technology	130 nm CMOS	2.5 µm CCD
Illumination	Back illumination	Back illumination
Optical thickness	~ 3 µm	10 – 250 µm
Peak QE	~ 55% (color filter)	~ 90 – 95%
Operating temp	Up to 50°C	-100°C – -140°C
Dark current	20 – 30 e-/pixel/sec	Few e-/pixel/hr
Read noise	~ 2 e-	~ 2-5 e-
Full well	~ 4500 e-	~ 200,000 e- (15 µm)
Cost	<< 	~ 

CCD 101 – Invention

- Invented by W. Boyle and G. Smith (Bell Laboratories) on September 8th, 1969 – Awarded Nobel Prize in Physics 2009
- Tasked by Jack Morton to find a semiconductor analogy to the magnetic "bubble memory"
- The basic concepts were conceived in a discussion session between Boyle and Smith "lasting not more than an hour" [1-3]

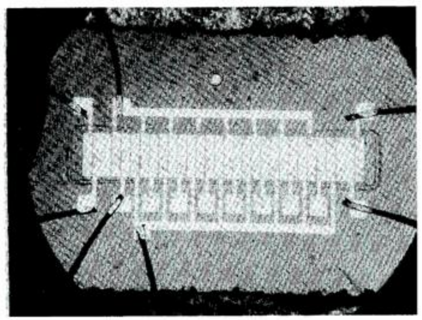

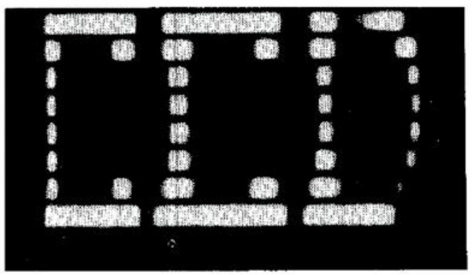

[1] G.E. Smith, "The invention and early history of the CCD," J. Appl. Phys., 109, 102421, 2011.
[2] W.S. Boyle and G.E. Smith, "The inception of charge-coupled devices," IEEE Trans. Elec. Dev., 23, 661, 1976.
[3] G.E. Smith, "The invention of the CCD", Nucl. Instrum. Meth. A, 471, 1, 2001.

CCD 101 – Boyle/Smith notebook entry

- Collection and storage of charge in MOS capacitor depletion regions
  - Dashed line denotes edge of depletion region
  - \+ denotes storage of charge (holes in this case)
- Charge transferred via clocking of closely spaced electrodes

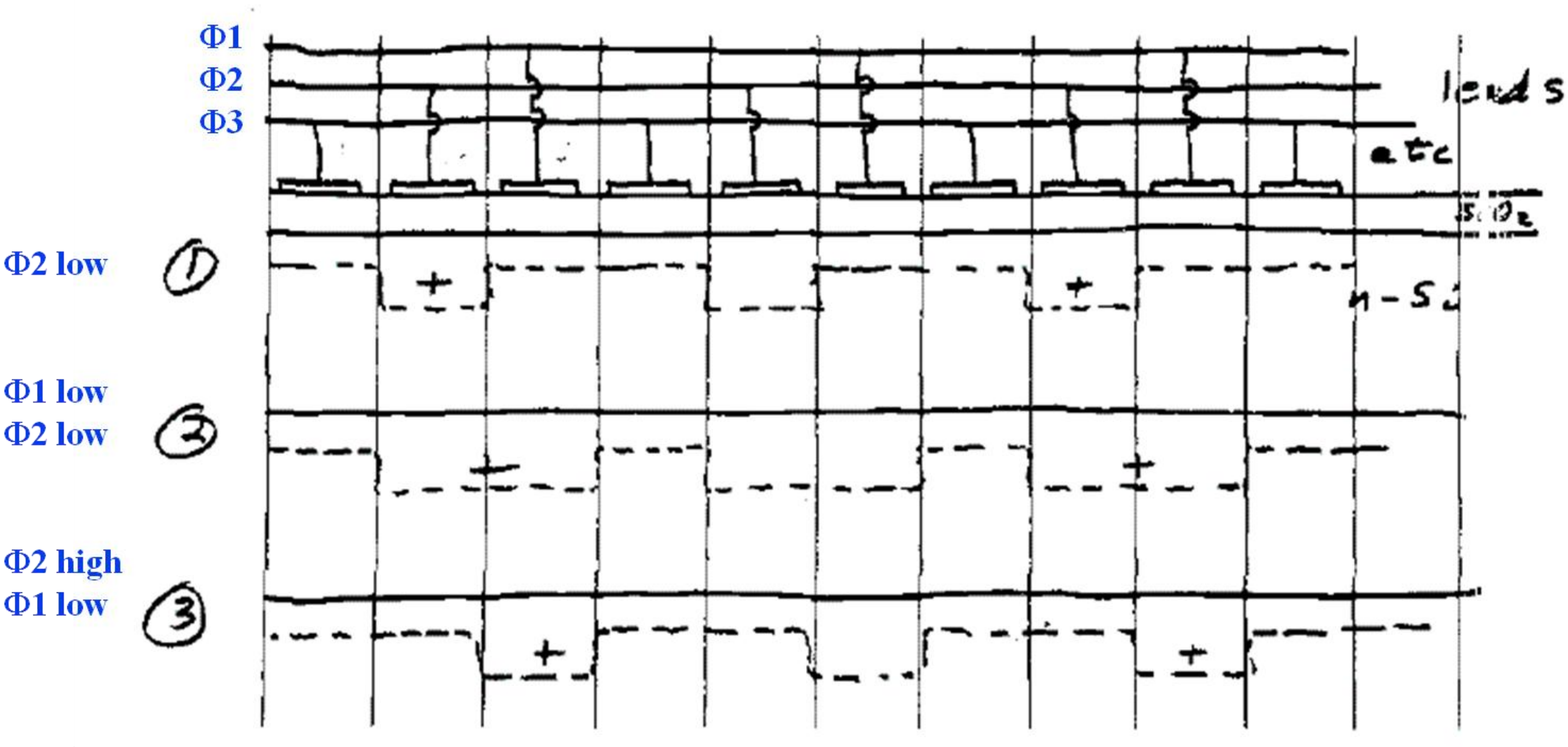

3-phase CCD diagram (lab notebook drawing Sept. 1969)

2D simulation of charge shift in CCD

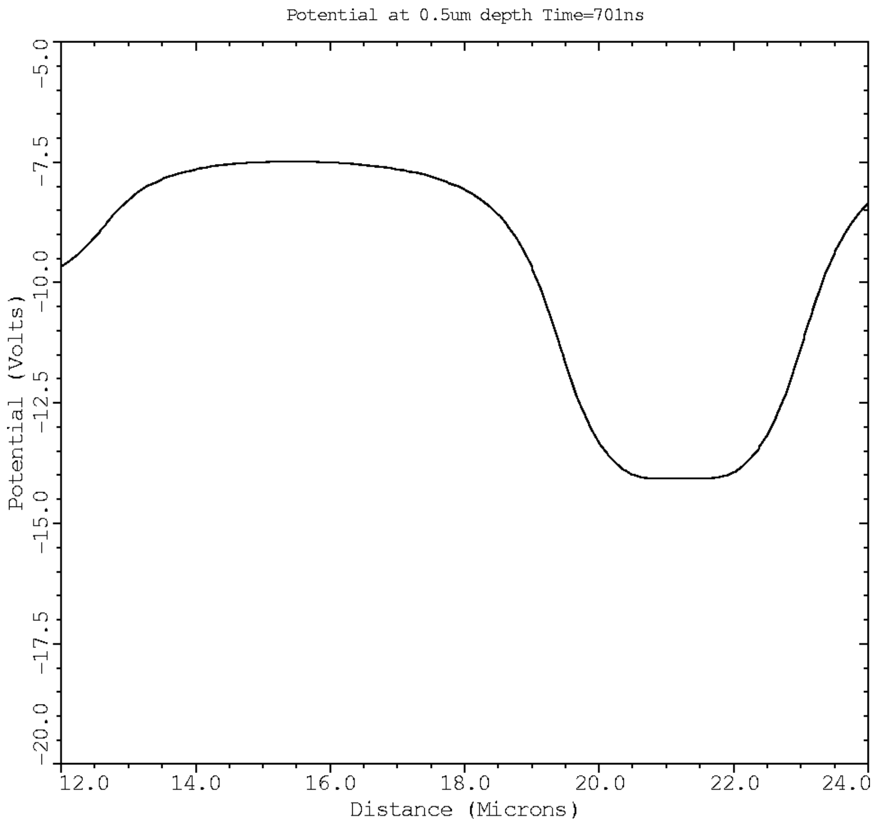

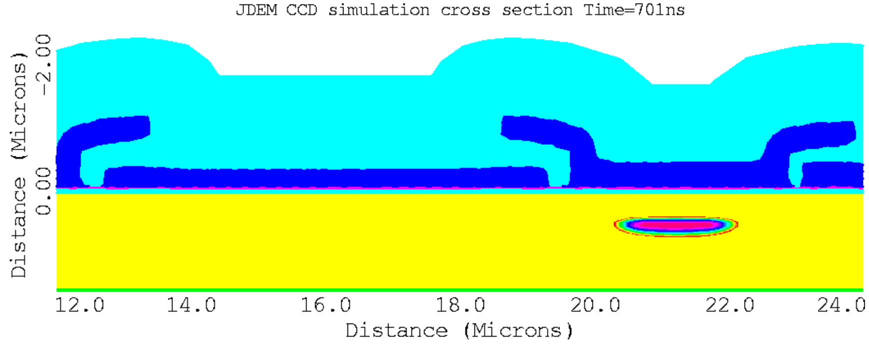

CCD 101 – Triple poly process

Scientific CCDs typically use the same 3-phase clocking as in the original Boyle and Smith concept with overlapping polysilicon gate electrodes (triple poly)

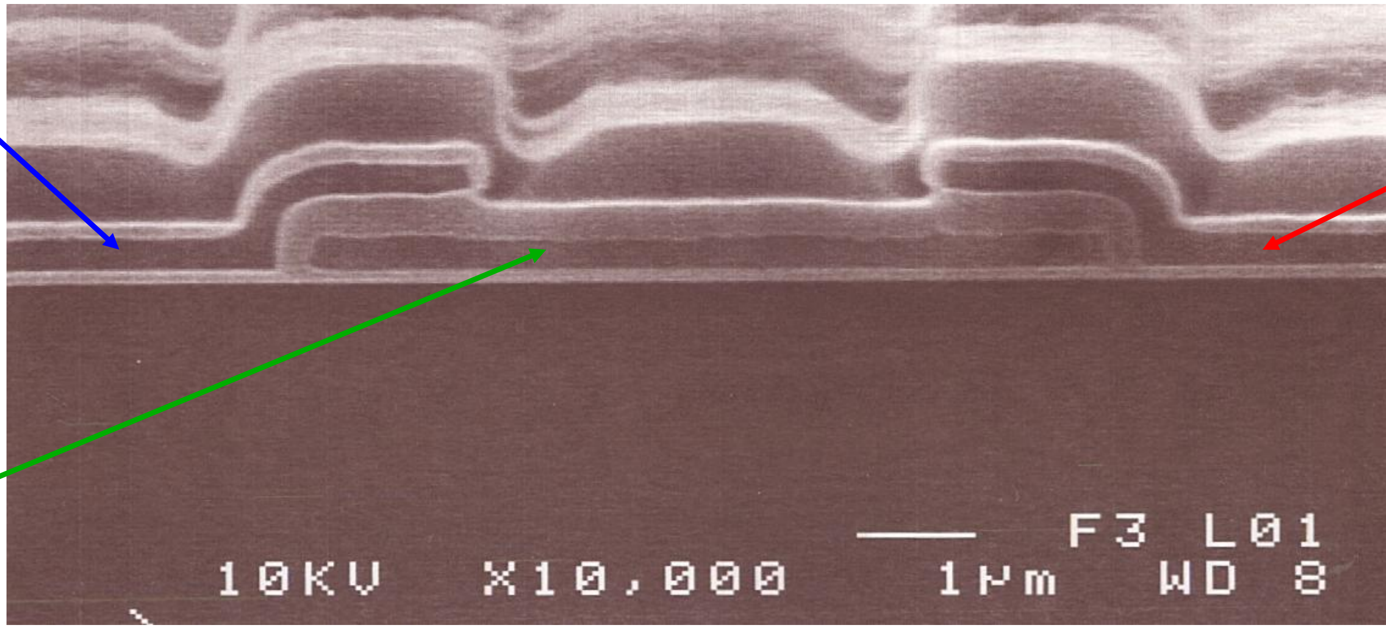

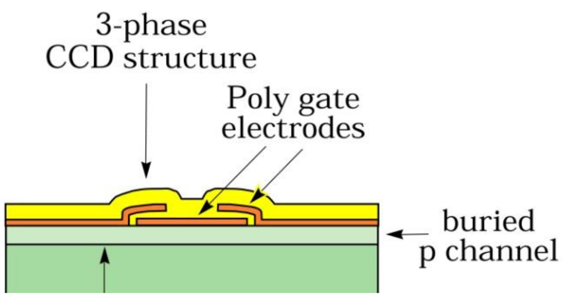

UC-Berkeley connections to CCD development

IEEE Trans. Elec. Dev., 21, 712, 1974

Charge-Coupled Area Image Sensor Using Three Levels of Polysilicon

CARLO H. SÉQUIN, MEMBER, IEEE, FRANCIS J. MORRIS, SENIOR MEMBER, IEEE, THEODORE A. SHANKOFF, MICHAEL F. TOMPSETT, MEMBER, IEEE, AND EDWARD J. ZIMANY, Jr.

Abstract—Charge-coupled area image sensors with 220 by 256 cells have been built using a three-phase overlapping electrode structure. Each of the three sets of electrodes is formed in a separate level of polysilicon which are isolated from each other by a thermally grown oxide. This approach relaxes the demands on mask making and photolithography that would otherwise be necessary and reduces the incidents of fatal shorts that render devices inoperable. The overlapping electrode structure results in stable performance and good transfer efficiency. The semitransparent polysilicon electrodes make the device usable with circuit side illumination although the spectral response is not very uniform. Average quantum efficiency in the visible part of the spectrum is 0.25. Measured resolution limits are 110 line pairs horizontally and 100 pairs vertically in accordance with present day PICTUREPHONE* specifications.

Manuscript received May 16, 1974.

C. H. Séquin, T. A. Shankoff, M. F. Tompsett, and E. J. Zimany are with Bell Laboratories, Murray Hill, N. J. 07974.
F. J. Morris is with Texas Instruments, Inc., Dallas, Tex. 75222.

INTRODUCTION

SOLID-STATE image sensors using the charge-coupled principle [1] were first constructed using a single level of metallization [2],[3]. In these devices a frame transfer organization [4] has been employed, in which the image is integrated in a separate imaging section and then, to prevent optical smearing, is quickly shifted in a parallel process along vertical columns into a storage area

* Registered service mark of American Telephone and Telegraph Company.

Carlo Sequin, UC-Berkeley Professor of Computer Science since 1977

Abstract—Charge-coupled area image sensors with 220 by 256 cells have been built using a three-phase overlapping electrode structure. Each of the three sets of electrodes is formed in a separate level of polysilicon which are isolated from each other by a thermally grown oxide. This approach relaxes the demands on mask making and photolithography that would otherwise be necessary and reduces the incidents of fatal shorts that render devices inoperable. The overlapping electrode structure results in stable performance and good transfer efficiency. The semitransparent polysilicon electrodes make the device usable with circuit side illumination although the spectral response is not very uniform. Average quantum efficiency in the visible part of the spectrum is 0.25. Measured resolution limits

Manuscript received May 16, 1974.
C. H. Séquin, T. A. Shankoff, M. F. Tompsett, and E. J. Zimany are with Bell Laboratories, Murray Hill, N. J. 07974.
F. J. Morris is with Texas Instruments, Inc., Dallas, Tex. 75222.

For maximum quantum efficiency scientific CCDs are back illuminated

Front vs Back illumination – CCDs

Front illumination: Quantum efficiency loss from

- Absorption in polysilicon gates
- Reflections from complicated thin film stack

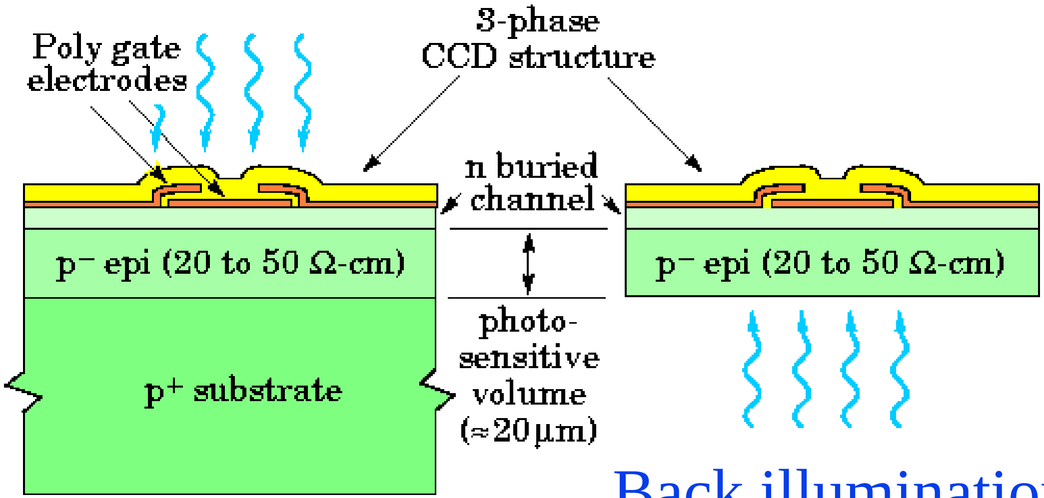

Back illumination (thinned CCDs):

- Remove p+ substrate
- Limited depletion depth for typical resistivity silicon implies significant thinning (10 – 20 µm for scientific CCDs, ~ 3 µm for CMOS image sensors)

Front vs Back illumination – CCDs

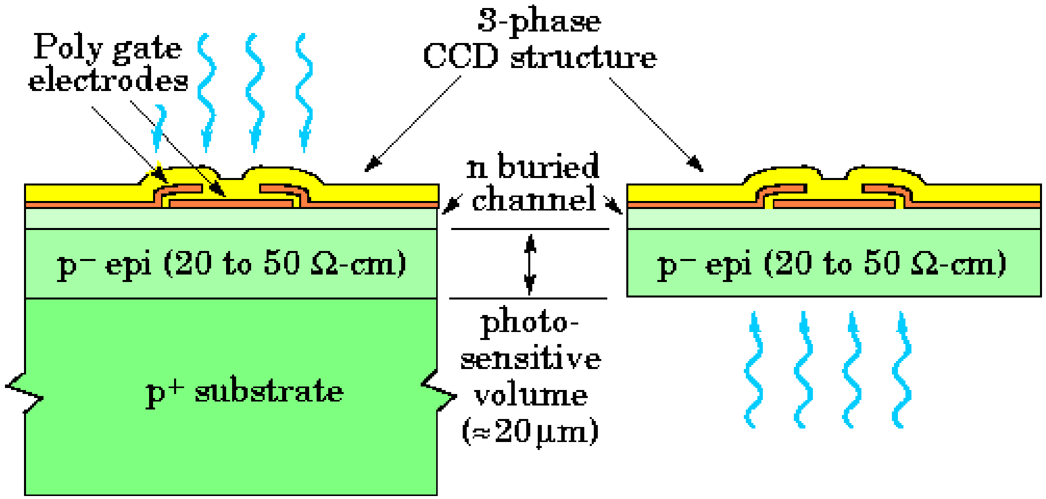

Sloan Digital Sky Survey
CCD quantum efficiency
versus wavelength comparing

1) **Back illumination**

2) **Front illumination**

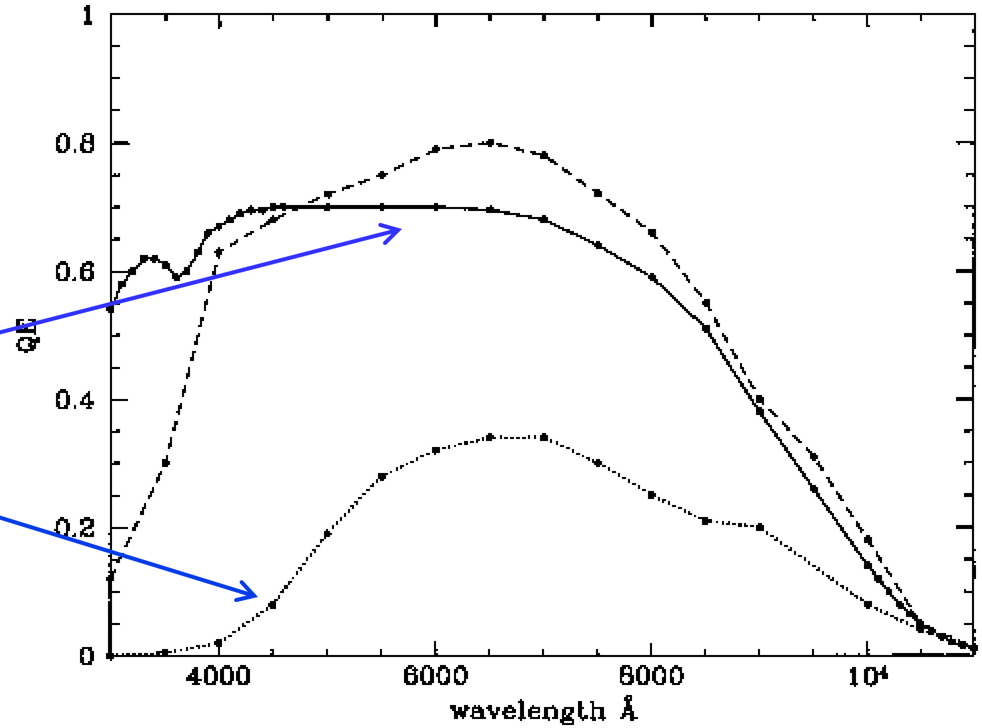

CCD vs CMOS image sensor

- CCDs: Shifting of charge vertically and horizontally to a source follower amplifier that converts charge to voltage
- CMOS image sensors have an SF amplifier in each pixel eliminating the need for high charge-transfer efficiency

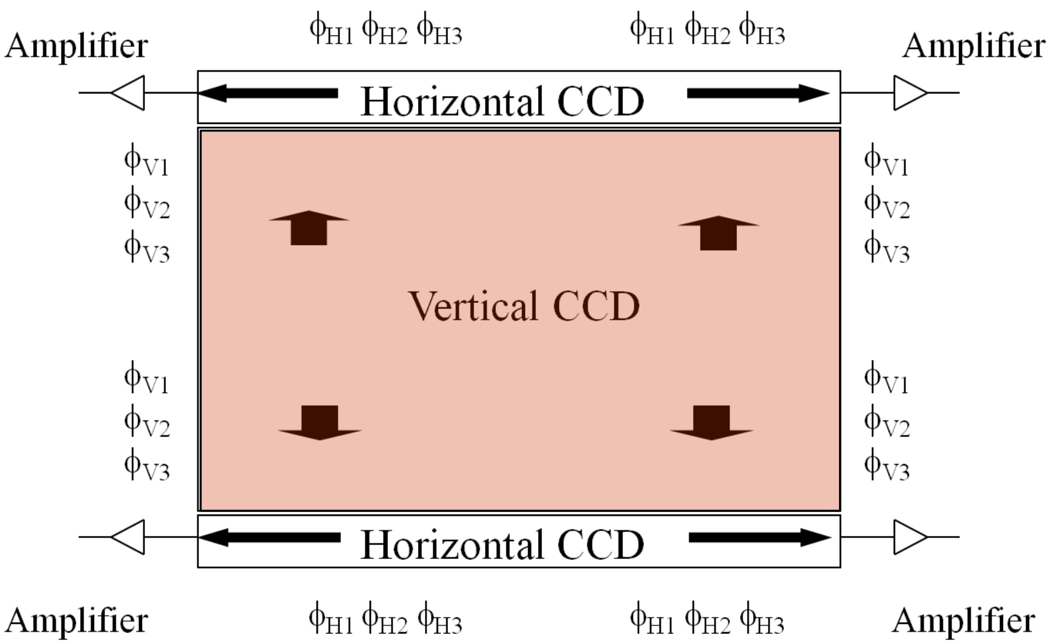

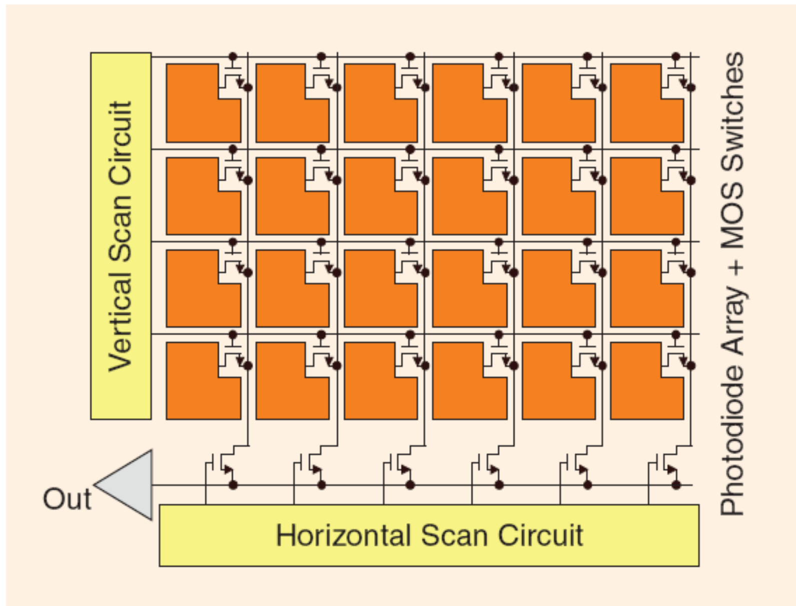

FIGURE 2: Architecture of a two-dimensional CMOS image sensor.

A. Theuwissen, IEEE Solid-State Circuits Magazine, 22, Spring 2010

CCD 101 – CMOS image sensor

- CMOS image sensors incorporate pinned photodiodes[1] to suppress surface dark current and floating diffusion amplifiers
  - kTC noise suppression – Borrowed from CCDs

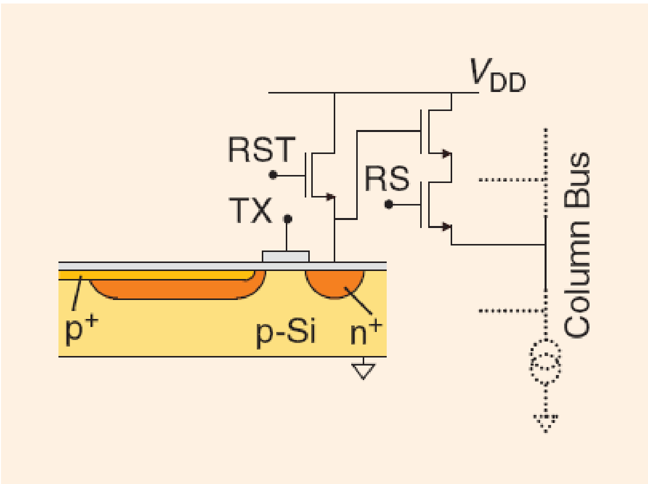

FIGURE 6: PPD CMOS pixel based on an in-pixel amplifier in combination with a PPD. RST, RS, and TX are respectively the reset, row select, and transfer transistors.

A. Theuwissen, IEEE Solid-State Circuits Magazine, 22, Spring 2010

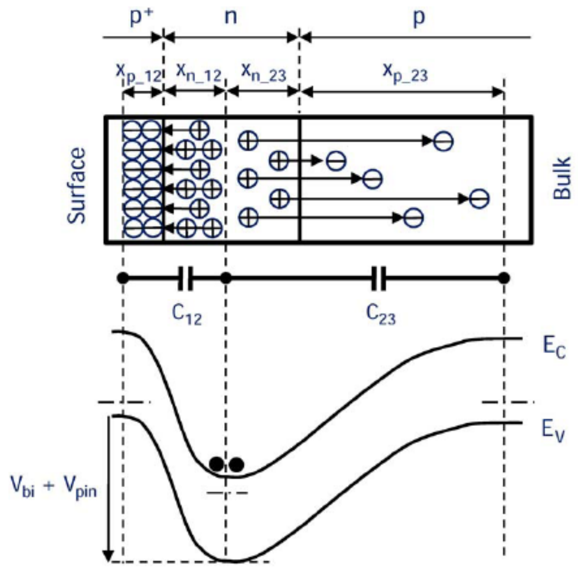

Analogous to buried channel CCD potential profile

Fig. 4. *Charge distribution and energy band diagram of the PPD. Signal charge excited by the incoming light can be accumulated in a potential well.* $C_{12} \propto (x_{p\_12} + x_{n\_12})^{-1/2}$, $C_{23} \propto (x_{n\_23} + x_{p\_23})^{-1/2}$.

Takayanagi and Nakamura, to appear in IEEE Proceedings

[1]N. Teranishi et al, IEEE Trans. Elec. Dev., **31**, 1829, 1984

Front vs back illumination – CMOS

- CMOS image sensors with small pixels need back illumination simply to get the light into the pixel

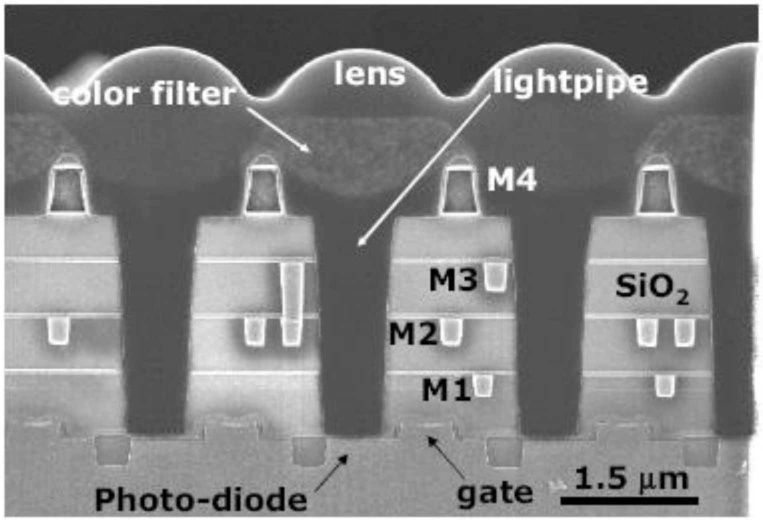

Fig. 3. SEM cross-section of 2.2 µm pixel with lightpipe and Cu wiring

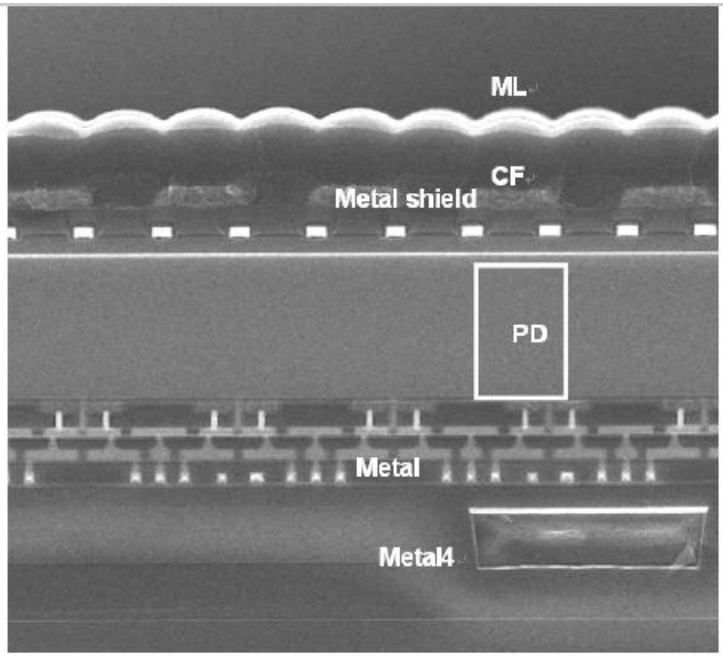

Figure 22.9.2: 1.65µm pixel cross-section.

IBM front illuminated CMOS image sensor
2.2 µm pixel
2006 IDEM (Gambino et al)

Sony back illuminated CMOS image sensor
1.65 µm pixel
2010 ISSCC (Wakabayashi et al)

Outline

- Fundamentals of CCDs and CMOS image sensors
- Scientific CCDs for astronomy
- Fully depleted CCDs fabricated on high-resistivity silicon – device physics/applications/technology

Scientific CCDs for Astronomy

- Scientific charge-coupled devices are the detector of choice for astronomy applications in the UV, visible and near-infrared wavelengths

λ ~ 350 nm to about 1.1 μm (atmospheric cutoff to Si bandgap)

— Back illuminated for high quantum efficiency

> 90% peak

— Slow readout for low noise

< 5 e- typically at 100 kpixels/sec readout

Scientific CCDs for Astronomy

- Scientific charge-coupled devices (cont')

—Cryogenically cooled for low dark current

Few electrons/pixel-hour at -100 to -140^{o}C

—Large format with large pixels

10 – 15µm pixels, 4k x 4k and larger

—Very $$$

Examples of astronomy cameras follow

CCD cameras for astronomy

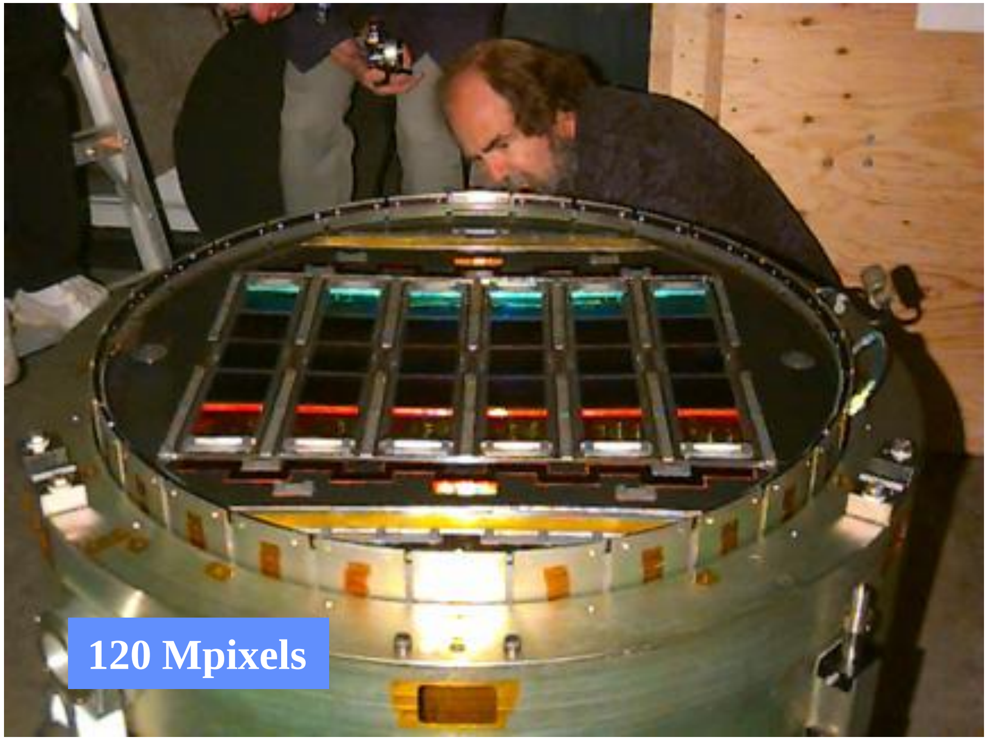

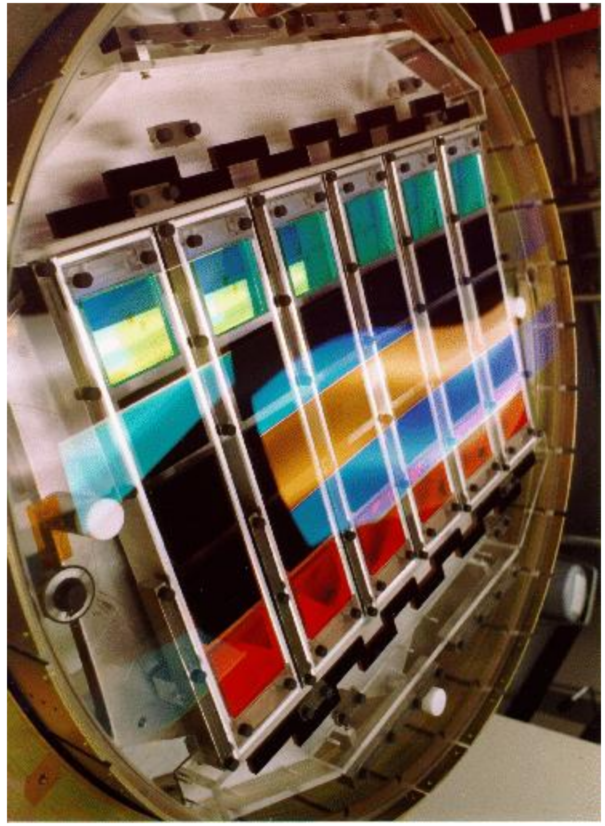

SDSS Photometric Camera – 30 2k x 2k, (24 μm)^2-pixel CCDs
Sloan Digital Sky Survey Telescope / 2000 – 2008

Thinned (~ 10 – 20 μm thick), partially depleted CCDs from SITe

CCD cameras for astronomy

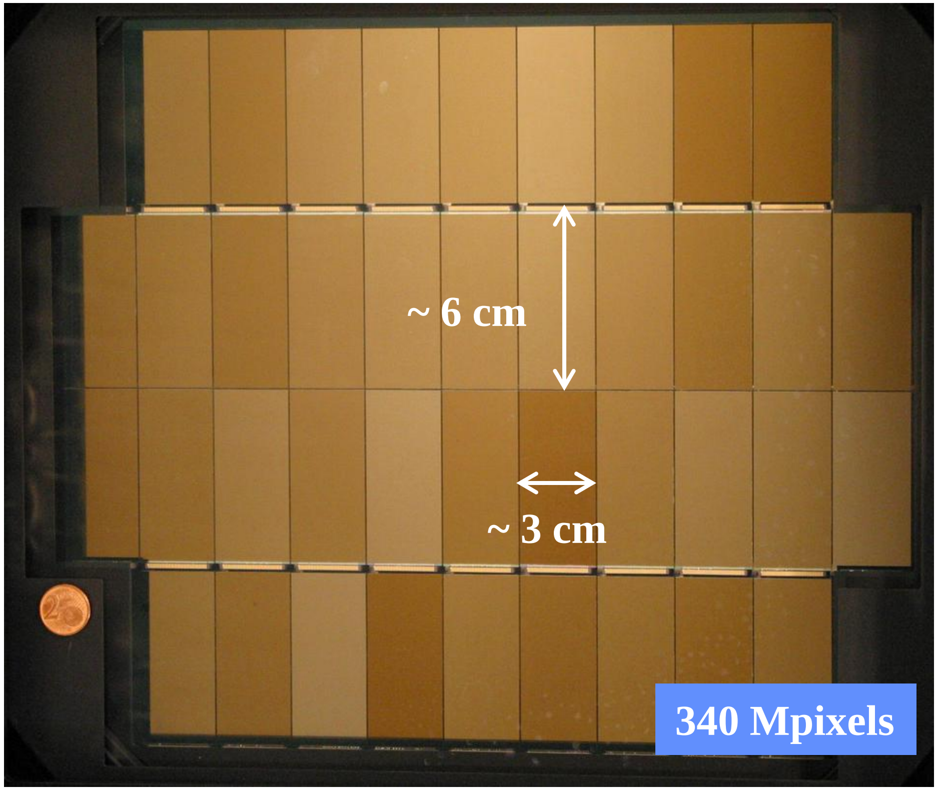

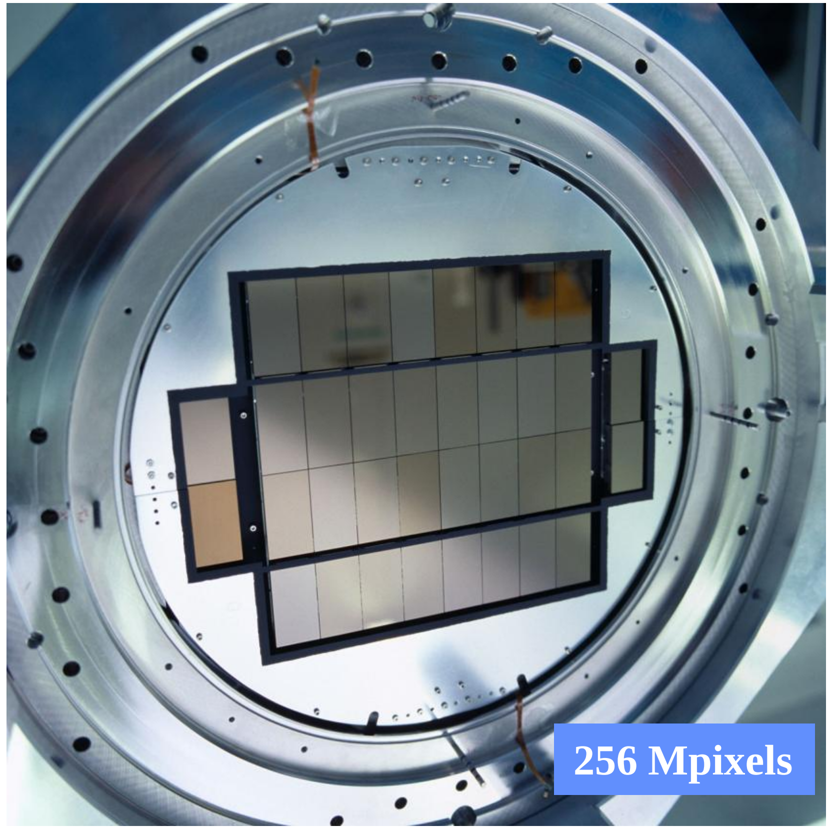

MegaCam – 36 2k x 4k, (15 µm)^2-pixel CCDs
Canada-France-Hawaii Telescope / 2003

OmegaCAM – 32 2k x 4k, (15 µm)^2-pixel CCDs
ESO VLT Survey Telescope (VST)
1st light June 2011

Thinned (~ 10 – 20 µm thick), partially depleted CCDs from e2V

CCD cameras for astronomy (cont')

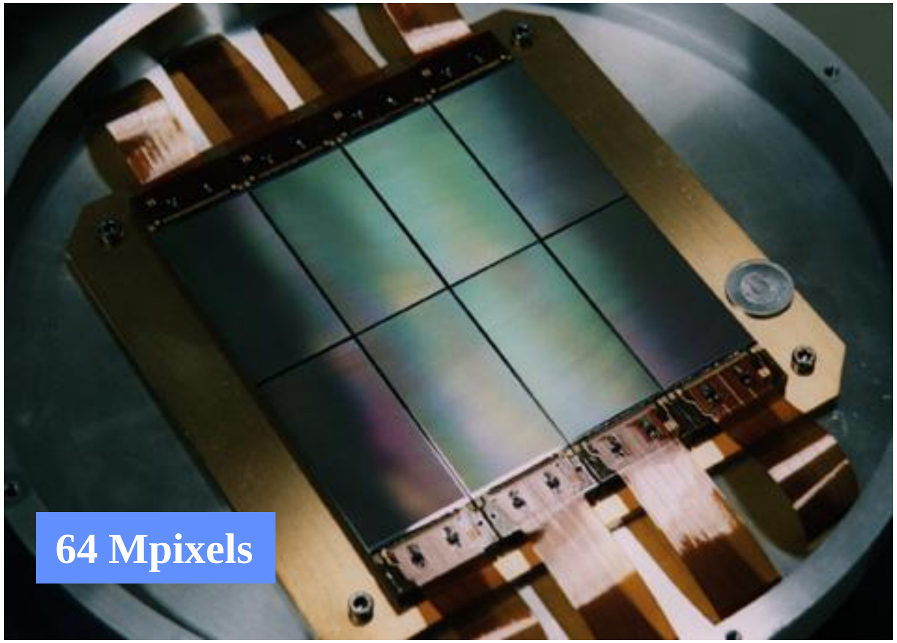

SuprimeCam – 8 2k x 4k, (15 μm)^2-pixel CCDs
Subaru 8-m Telescope (1998)

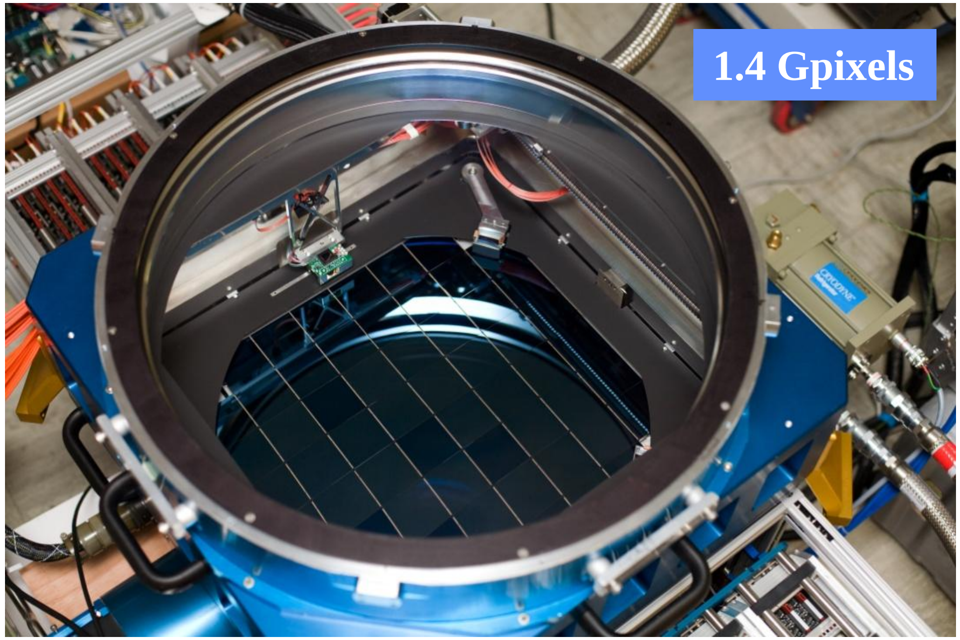

PS1 camera – 60 4.8k x 4.8k, (10 μm)^2-pixel CCDs
Pan-STARRS telescope (2010)

~ 40 μm thick, partially depleted and ~ 75 μm thick, fully depleted CCDs
(deep depletion CCDs)

MIT Lincoln Laboratory

CCD cameras for astronomy (cont')

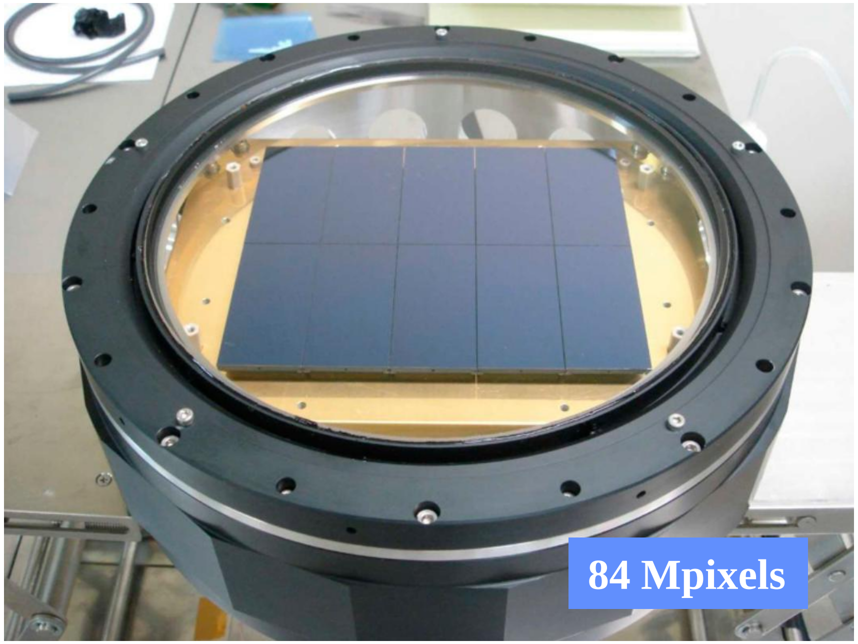

SuprimeCam – 10 2k x 4k, (15 μm)^2-pixel CCDs
Subaru 8-m Telescope (2008)

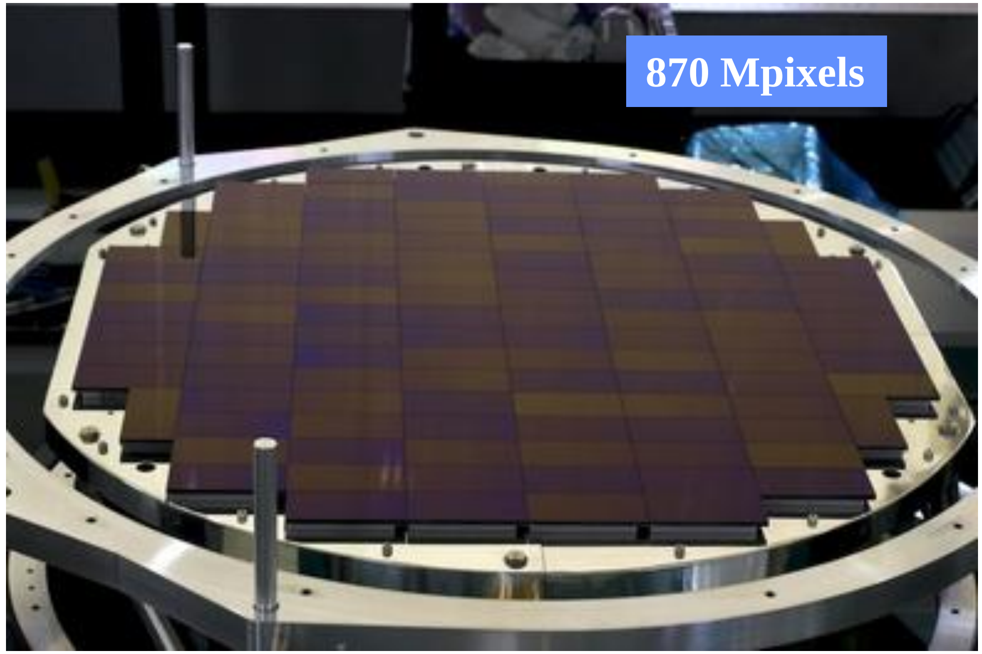

HyperSuprimeCam – 116 2k x 4k, (15 μm)^2-pixel CCDs
Subaru 8-m Telescope
1st light achieved 28Aug2012

~ 200 μm thick, fully depleted CCDs

Hamamatsu Corporation

Coming soon – Fermi National Accelerator Laboratory Dark Energy Survey Camera

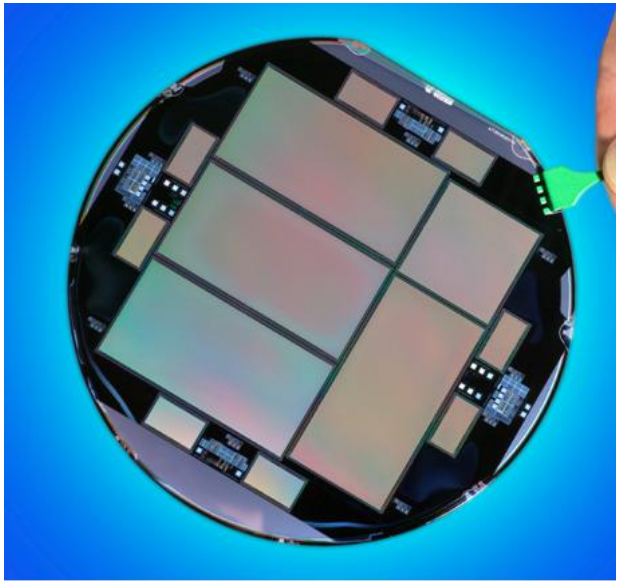

Dark Energy Survey Camera (DECam) – 62 2k x 4k, (15 μm)^2-pixel CCDs

NOAO Cerro Tololo Blanco 4-m Telescope (Fall 2012)

250 μm thick, fully depleted CCDs (DALSA/LBNL)

Coming soon – Fermi National Accelerator Laboratory Dark Energy Survey Camera

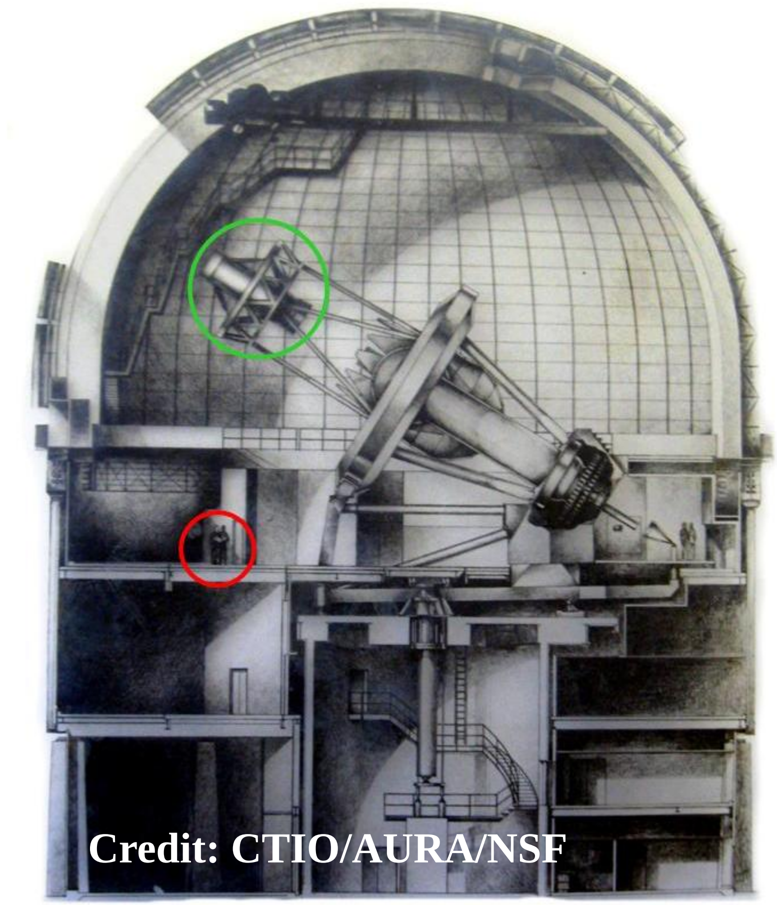

Artist's rendering – Cerro Tololo Inter-American Observatory V. M. Blanco 4-m telescope (Chile)

Coming soon – Fermi National Accelerator Laboratory Dark Energy Survey Camera

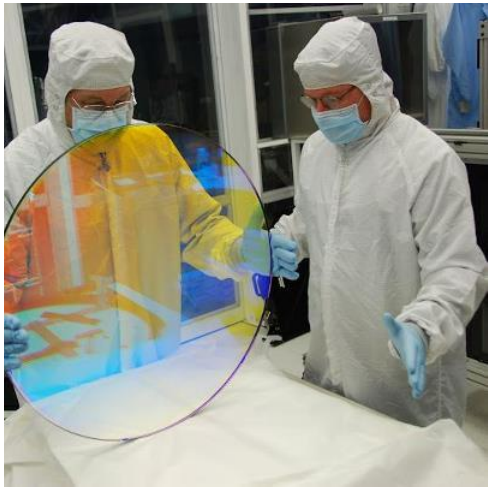

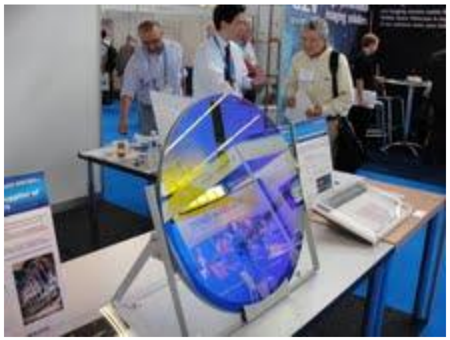

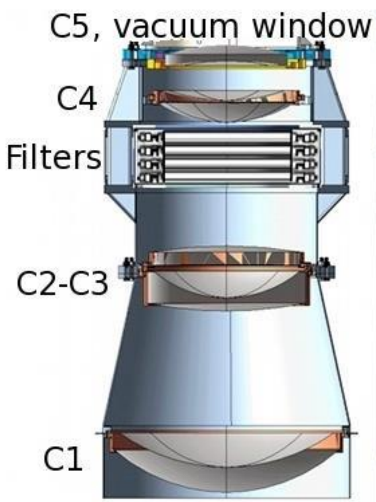

DECam barrel and optics

Credit:
CTIO/NOAO
AURA/NSF

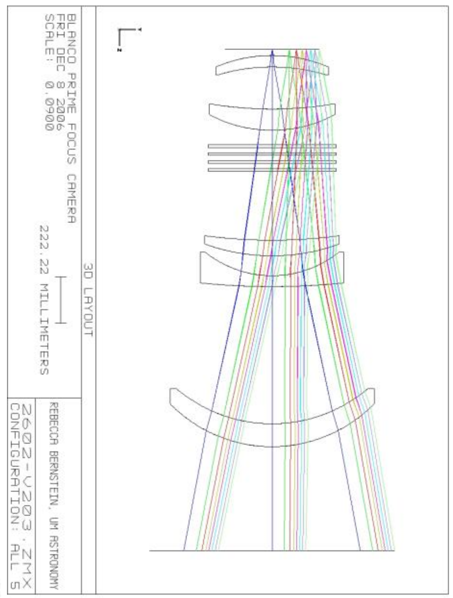

Coming soon – Fermi National Accelerator Laboratory Dark Energy Survey Camera

DECam's imager is visible for the last time (blue, left of center) before it is inserted into the instrument, meeting the optical corrector for the first time.
Image credit: T. Abbott CTIO/NOAO/AURA.

DES Collaboration

… is an international project to "nail down" the dark energy equation of state.

Fermilab, UIUC/NCSA, University of Chicago, LBNL, NOAO, University of Michigan, University of Pennsylvania, Argonne National Laboratory, Ohio State University, Santa-Cruz/SLAC Consortium, Texas A&M

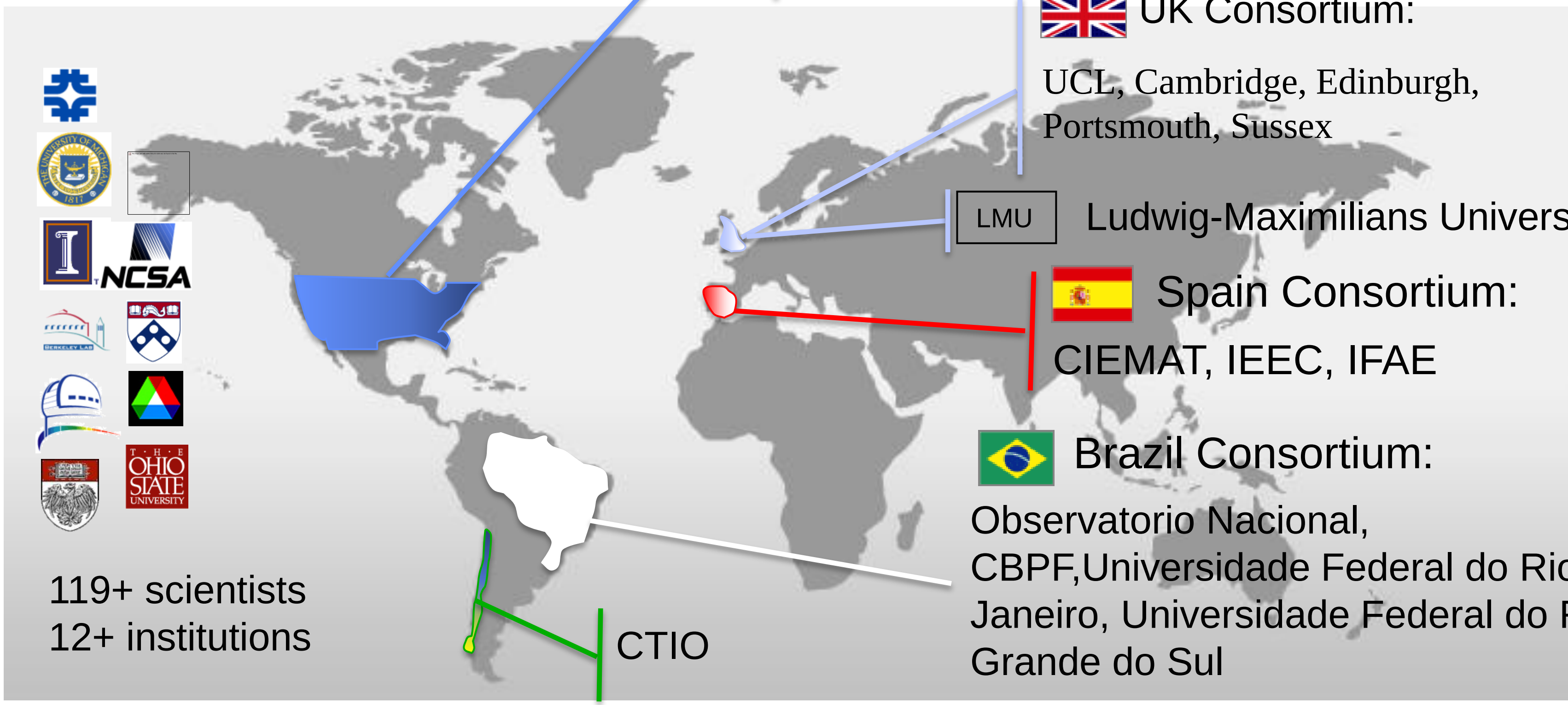

Outline

- Fundamentals of CCDs and CMOS image sensors
- Scientific CCDs for astronomy
- Fully depleted CCDs fabricated on high-resistivity silicon – **device physics**/applications/technology

Fully depleted, back-illuminated CCD

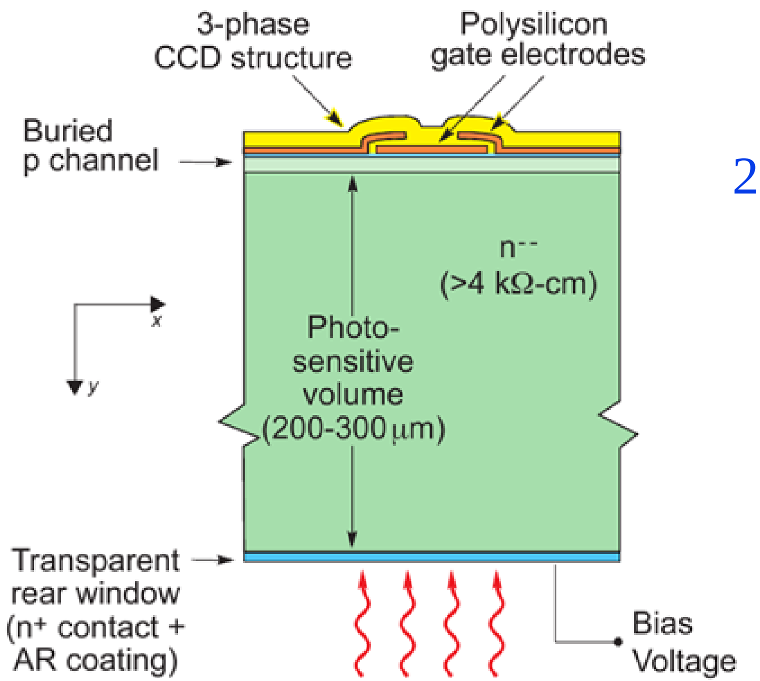

1) Concept: Fabricate a conventional CCD on a thick, high-resistivity Si substrate (> 4 kΩ-cm)
   - 200-250 μm typical

2) Use a substrate bias voltage to fully deplete the substrate of mobile charge carriers
   - Merging of p-i-n and CCD technology
   - High-ρ Si allows for low depletion voltages
   - <u>Float-zone refined silicon</u>

High-resistivity silicon 101

Standard silicon is produced by the Czochralsky method:

The ingot is pulled from molten silicon starting from a seed crystal

The crucible is lined with quartz, which results in oxygen incorporation into the silicon

Oxygen donors limit the resistivity to about 50 Ω-cm

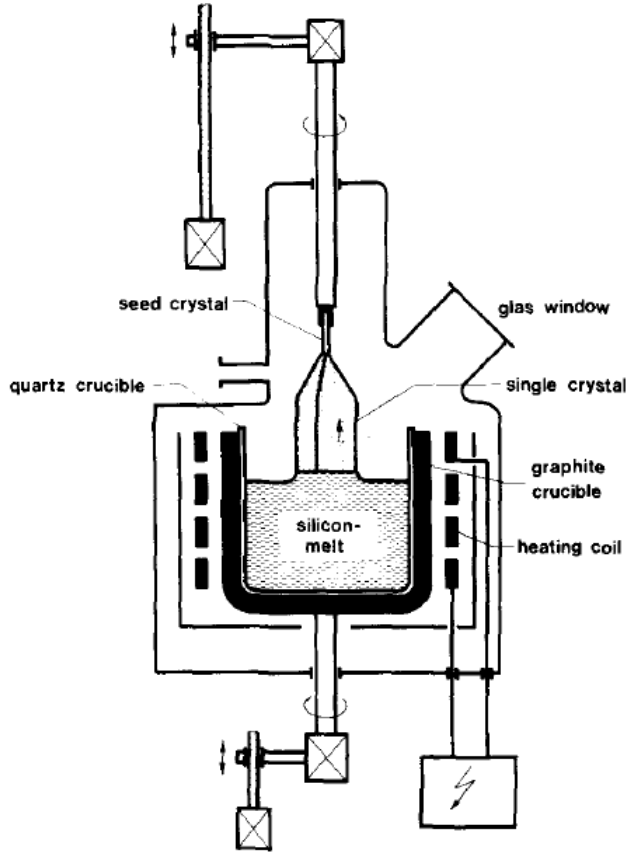

Fig. 3. Single crystal growth by the Czochralsky technique.

94

Nuclear Instruments and Methods in Physics Research 226 (1984) 94–102
North-Holland, Amsterdam

THE PRODUCTION AND AVAILABILITY OF HIGH RESISTIVITY SILICON FOR DETECTOR APPLICATION

Wilfried von AMMON and Heinz HERZER

Wacker-Chemitronic GmbH, 8263-Burghausen, Fed. Rep. Germany

The production of detector-grade silicon is briefly reviewed. Material parameters such as bulk resitivity, radial resistivity variation and compensation, as well as wafer geometry are discussed with respect to what a silicon manufacturer can supply.

High-resistivity silicon 101

High-resistivity silicon is produced by float-zone refining:

The ingot is locally melted by an RF heating coil that surrounds the ingot

Most impurities tend to segregate into the liquid phase

Repeated passes along the ingot drives the impurities to one end of the ingot

10 kΩ-cm corresponds to $N_D \sim 4.3 \times 10^{11}$ cm^{-3}
Equivalent to purity level of 1 part in 10^{11}

Depletion voltage is proportional to N_D

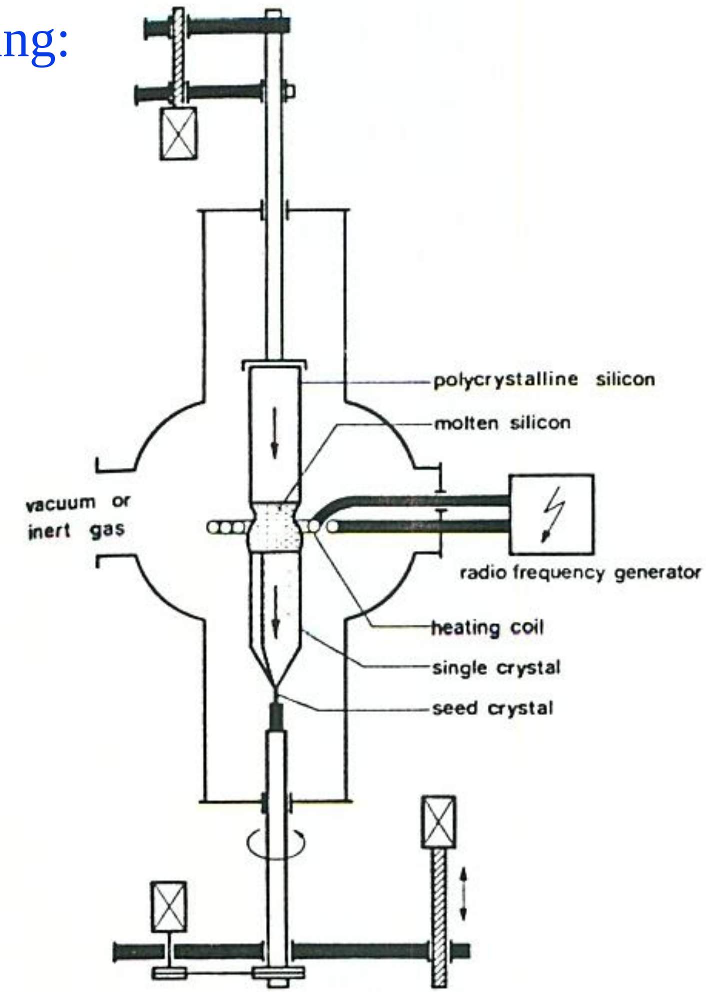

W. Von Ammon and H. Herzer, "The production and availability of high-resistivity silicon for detector application," Nucl. Instrum. Meth., **A226**, pp. 94-102, 1984

Fully depleted, back-illuminated CCD

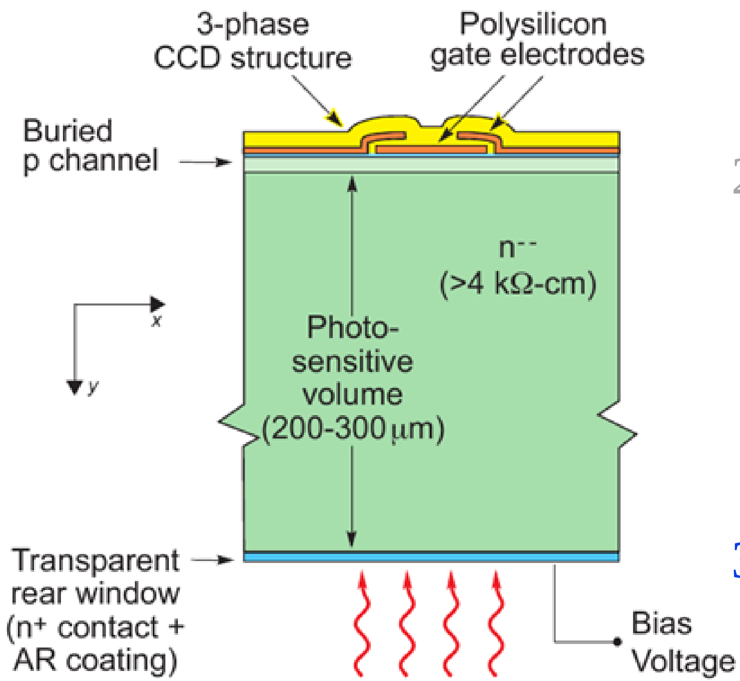

1) Concept: Fabricate a conventional CCD on a thick, high-resistivity Si substrate (> 4 kΩ-cm)
   - 200-250 μm typical, 500 μm in special cases

2) Use a substrate bias voltage to fully deplete the substrate of mobile charge carriers
   - Merging of p-i-n and CCD technology
   - High-ρ Si allows for low depletion voltages
   - Float-zone refined silicon

3) The large thickness results in high near-infrared quantum efficiency and greatly reduced fringing

Fully depleted, back-illuminated CCD

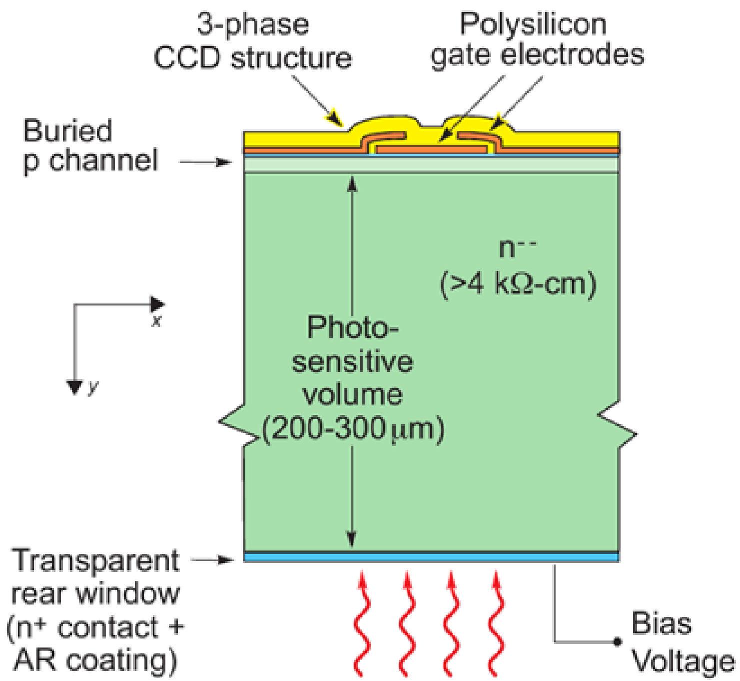

$$Photon\ Energy\ (eV) = \frac{1.24}{\lambda(\mu m)}$$

The wavelength cut-off in silicon due to the bandgap (~ 1.1 eV) is about 1.1 µm

Following plot includes the silicon absorption length that is defined as the inverse of the absorption coefficient α

$$I(x) = I_o \exp[-\alpha x]$$

Intensity of incident light

Quantum efficiency

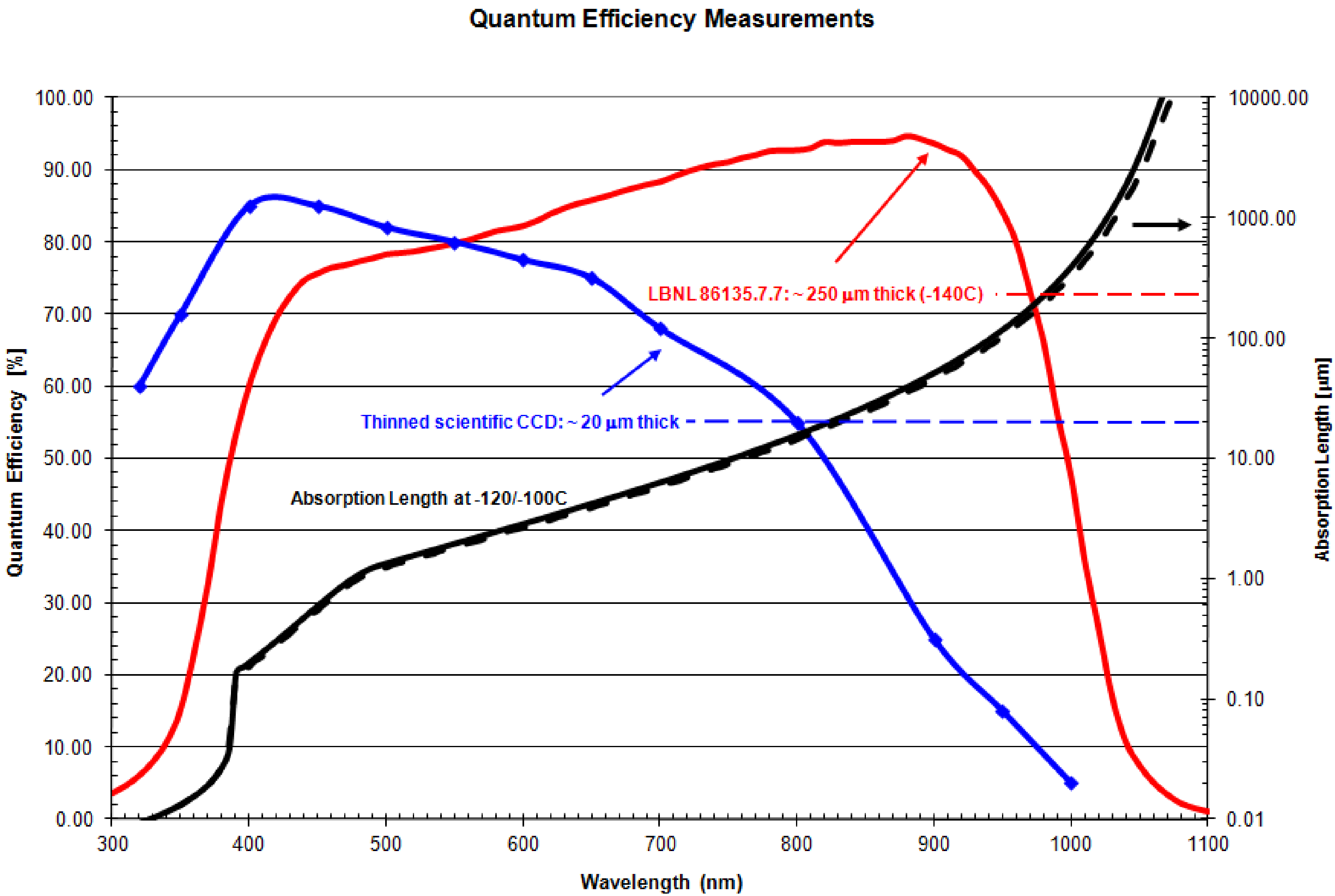

Quantum efficiency

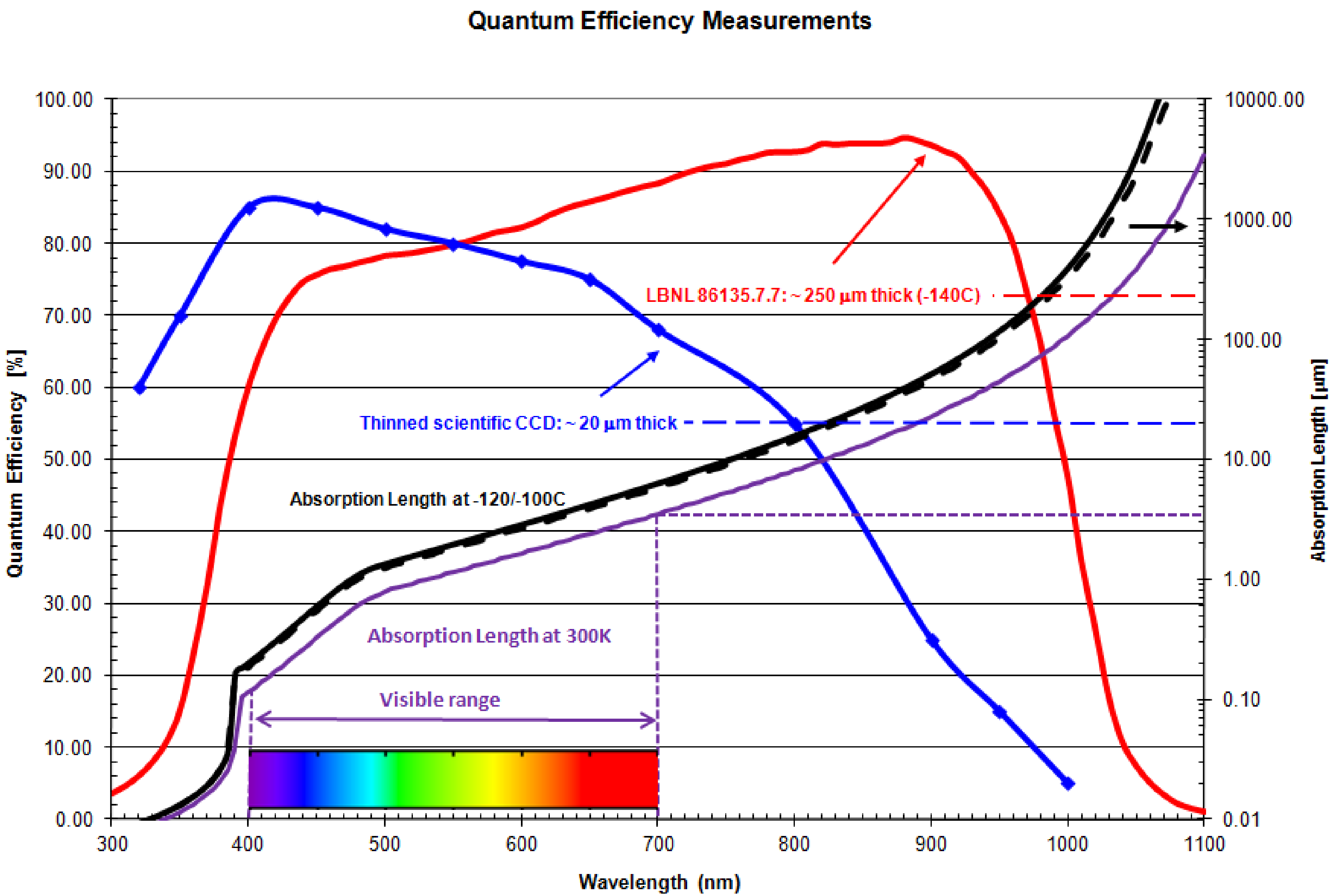

Visible range is 400 – 700 nm

Fully depleted, back-illuminated CCD

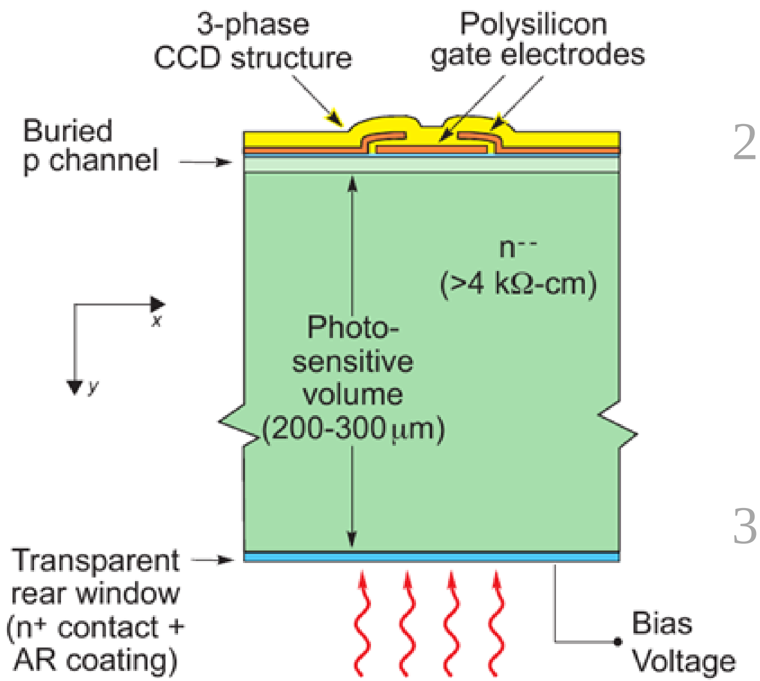

1) Concept: Fabricate a conventional CCD on a thick, high-resistivity silicon substrate
   - 200-250 μm typical, 500 μm in special cases

2) Use a substrate bias voltage to fully deplete the substrate of mobile charge carriers
   - Merging of p-i-n and CCD technology
   - High-ρ Si allows for low depletion voltages
   - Float-zone refined silicon

3) The thickness results in high near-infrared quantum efficiency and greatly reduced fringing

4) The fully depleted operation results in the ability to control the spatial resolution via the thickness and the substrate bias voltage

Fully depleted, back-illuminated CCD

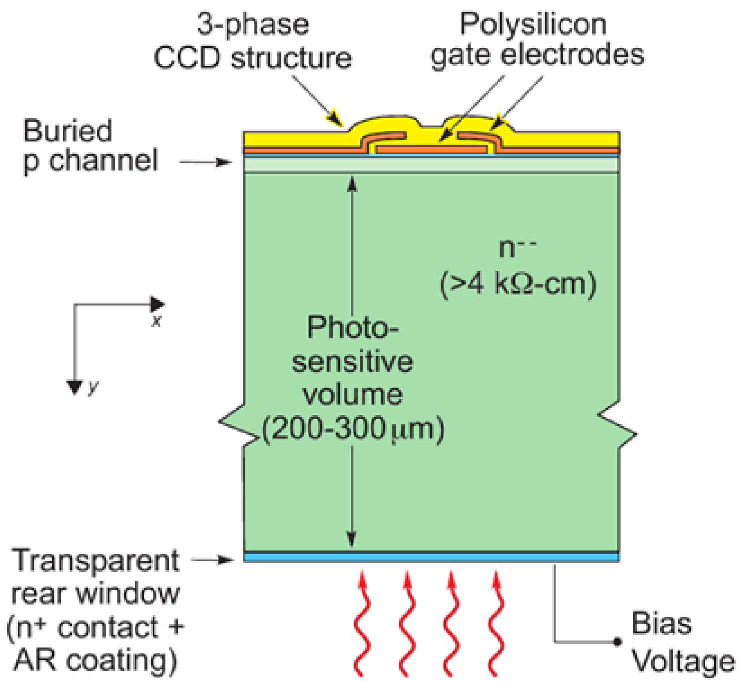

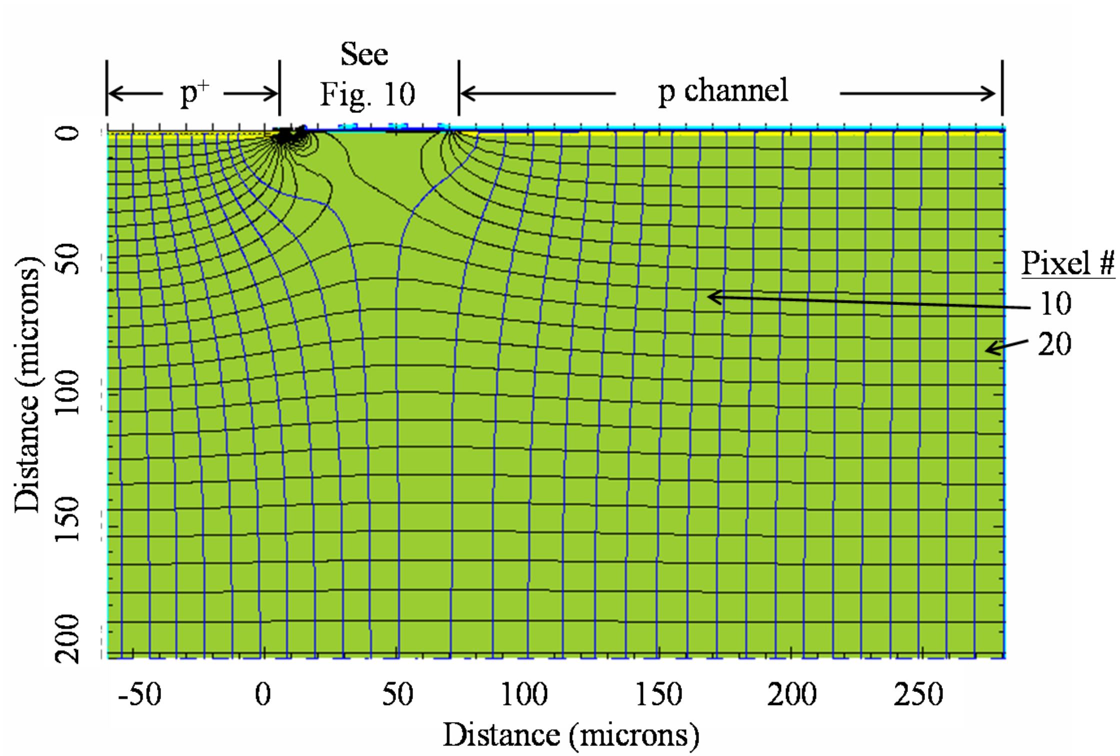

Note: Cross-section is not to scale

2D simulation – vertical field lines on right at pixel pitch of 10.5 μm

Spatial resolution: Effect of substrate voltage

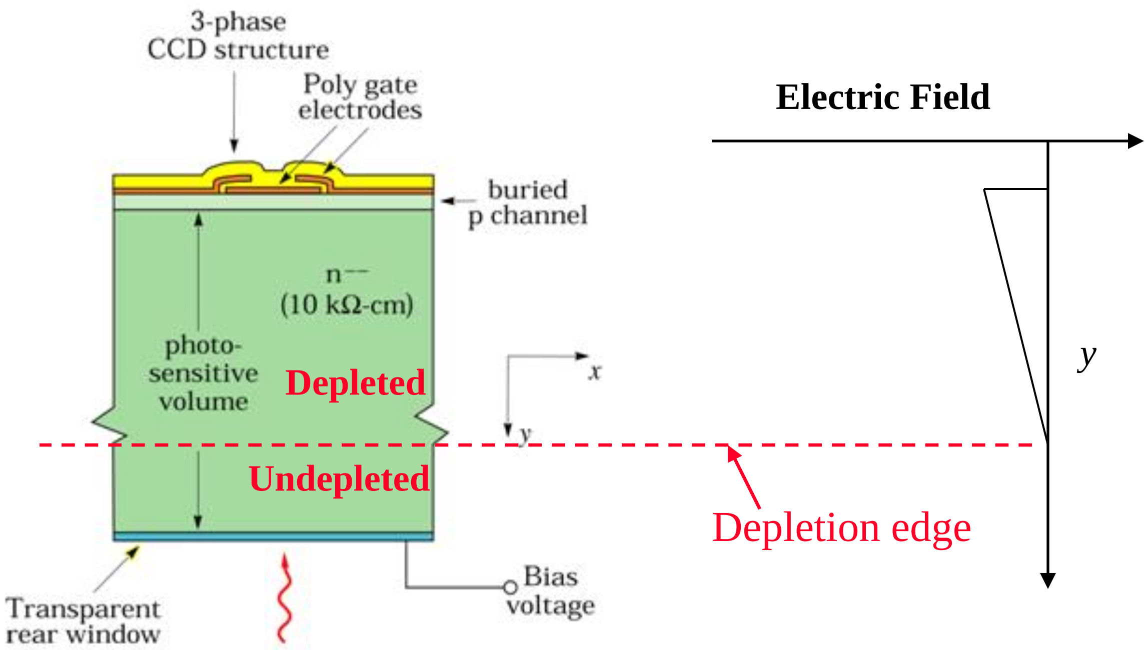

Point source illumination

V_{SUB} = 5V

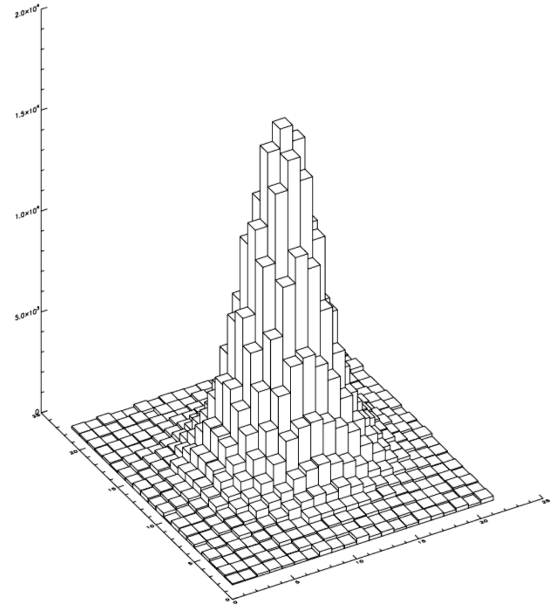

Measured charge distribution
Each square represents 1 pixel

At low substrate bias voltages the CCD is not fully depleted

The PSF is dominated by diffusion in the undepleted silicon
Can be shown that σ ~ the field-free region thickness

Spatial resolution: Effect of substrate voltage

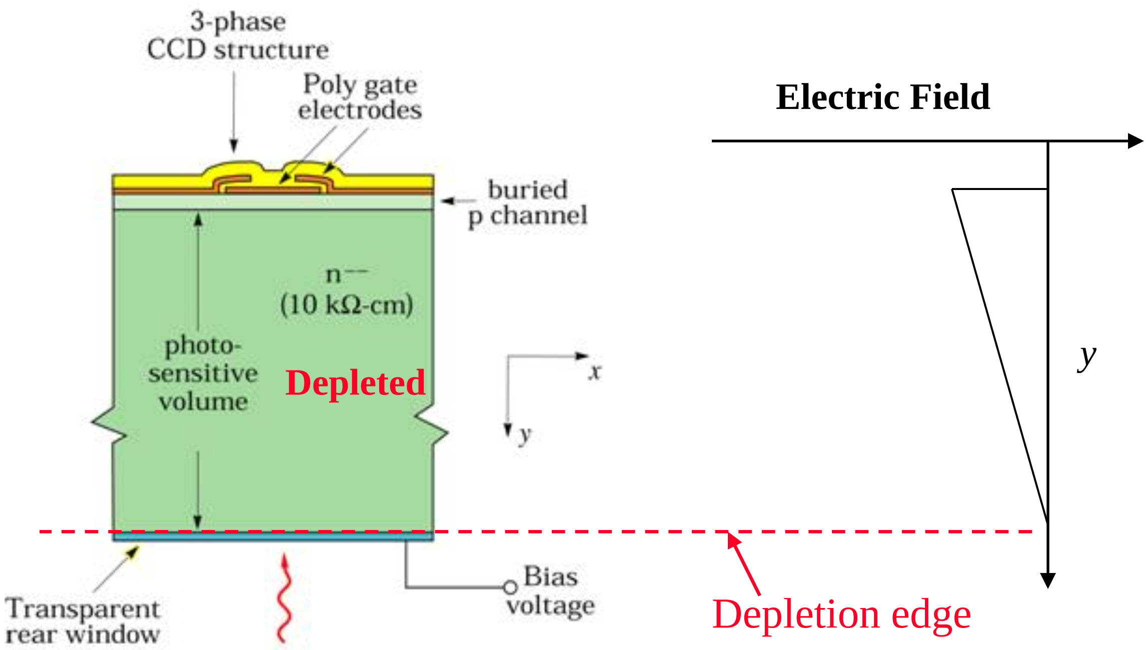

Point source illumination

$V_{SUB} = 20V$

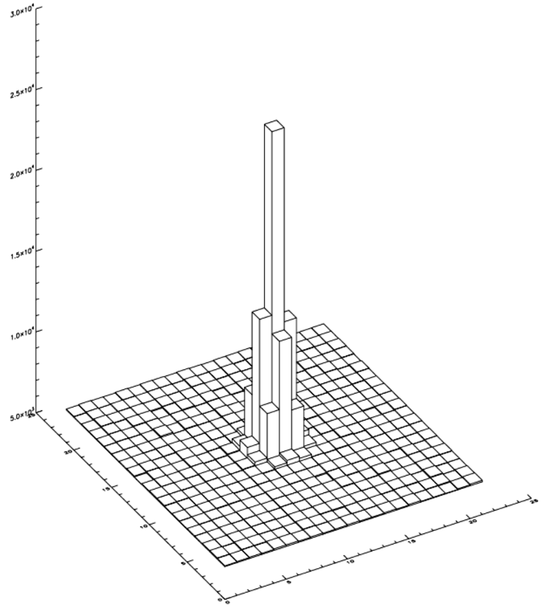

Measured charge distribution
Each square represents 1 pixel

At 20V the CCD corresponding to the data is just fully depleted

The PSF is limited by the transit time of the photogenerated holes

$$\sigma = \sqrt{2Dt_{tr}}$$

Spatial resolution: Effect of substrate voltage

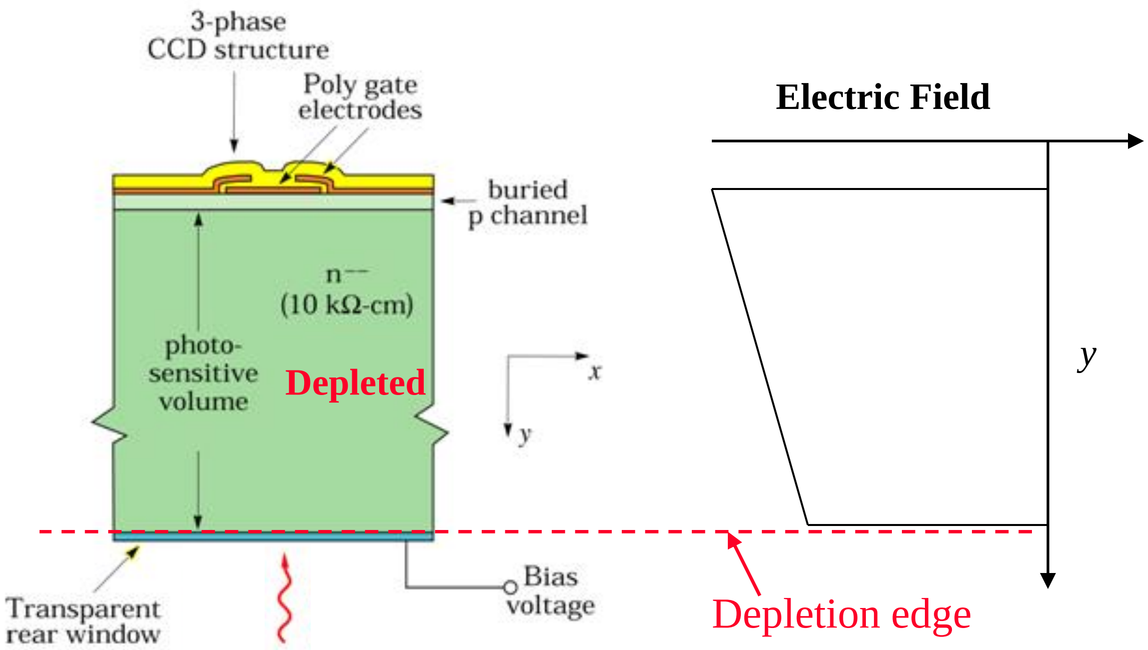

Point source illumination

V_{SUB} = 115V

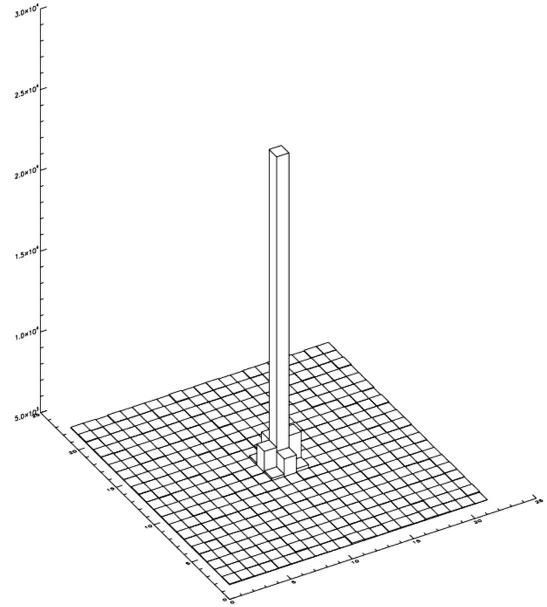

Measured charge distribution
Each square represents 1 pixel

The PSF continues to improve (but slowly) as V_{SUB} in increased

At V_{SUB}=115V the rms diffusion for this 200 µm thick,
10.5 µm pixel CCD is 3.7 ± 0.2 µm

Fully depleted, back-illuminated CCD

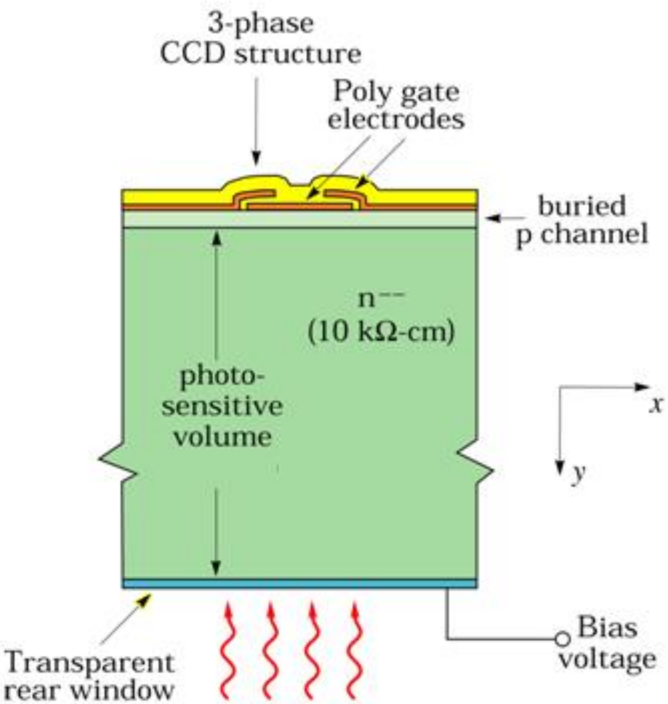

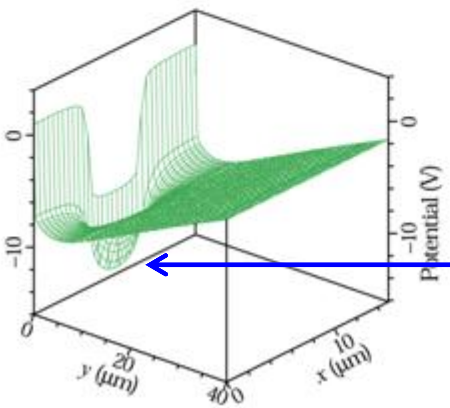

MEDICI 2-D simulation

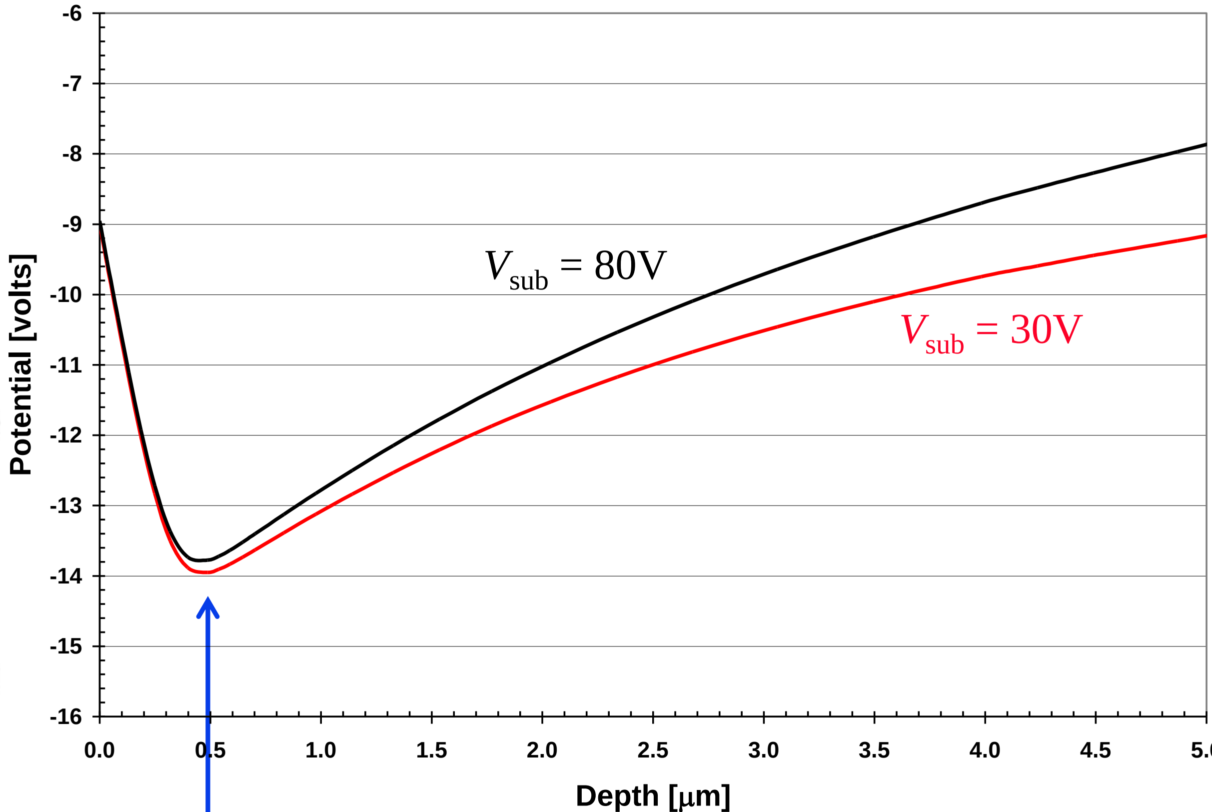

Potential minimum
(collecting phase)

MEDICI simulations

The value of the CCD potential minimum, where holes are collected, is not a strong function of the substrate bias voltage. As a result thick CCDs can operate over a wide range of substrate bias voltages.

Drawbacks of thick, fully depleted CCDs

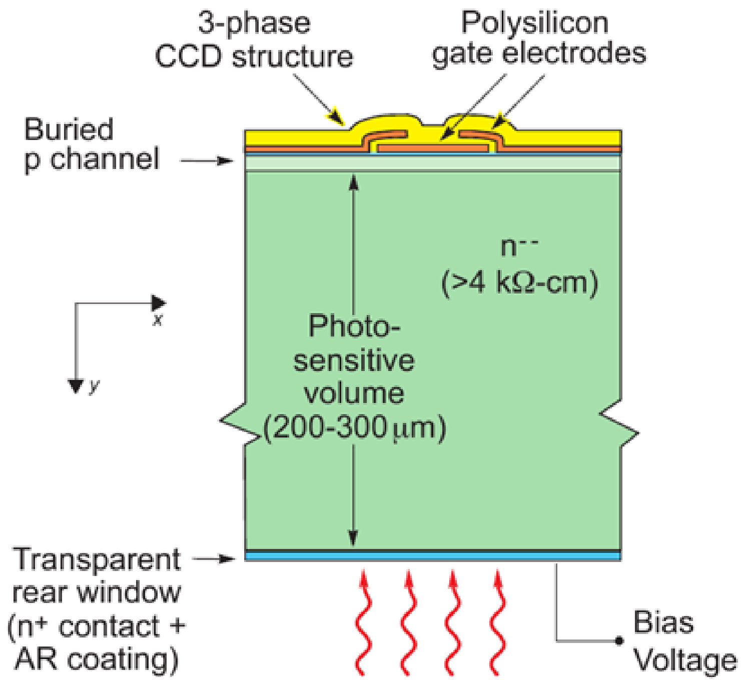

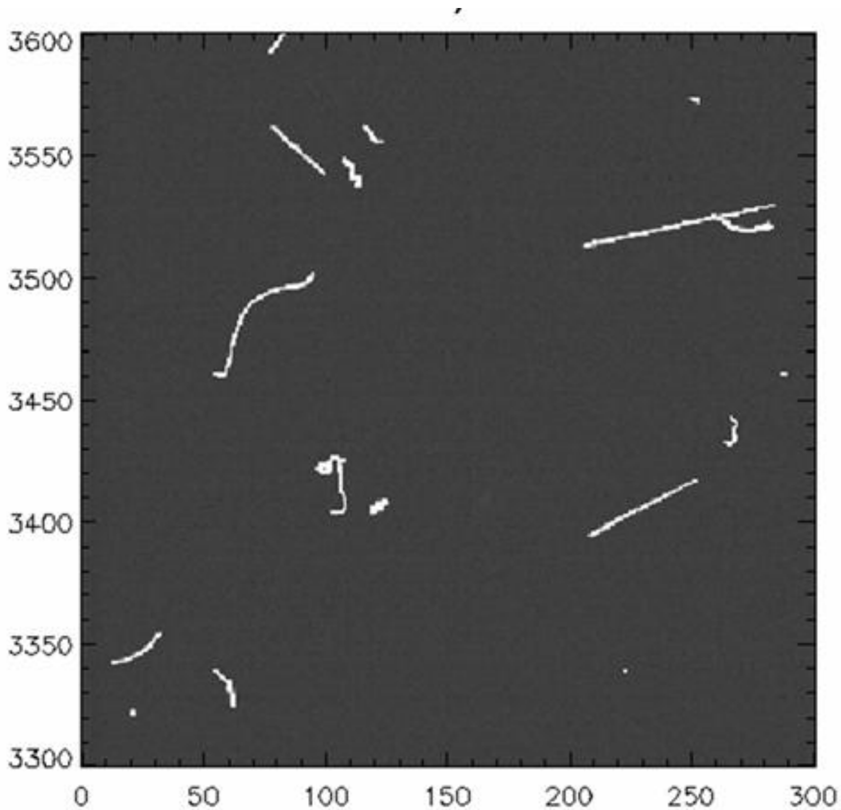

1) Cosmic rays and Compton electrons from background radiation leave long tracks

30 minute dark
200 μm thick CCD
Small sub-image

2) Degradation of spatial resolution at long wavelengths in fast optical systems where the light is incident at large angles

Outline

- Fundamentals of CCDs and CMOS image sensors
- Scientific CCDs for astronomy
- Fully depleted CCDs fabricated on high-resistivity silicon – device physics/**applications**/technology

Importance of near-IR response

Why is near-infrared response important?

Light from distant astronomical objects is shifted to longer wavelengths due to the expansion of the Universe

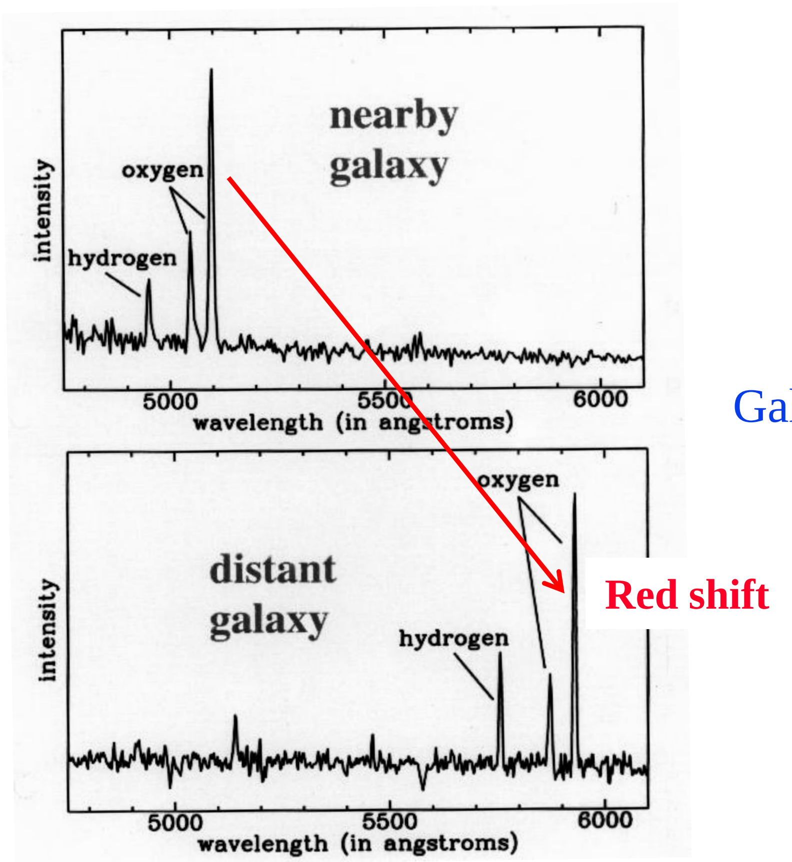

Galaxy spectra measured with CCDs

Importance of near-IR response

Why is near-infrared response important?

Light from distant astronomical objects is shifted to longer wavelengths due to the expansion of the Universe

$$z \equiv \frac{\lambda_{observed}}{\lambda_{at\,emission}} - 1 = \frac{v}{c} = \frac{Hd}{c}$$

Hubble's Law

Hubble & Humason (1931)

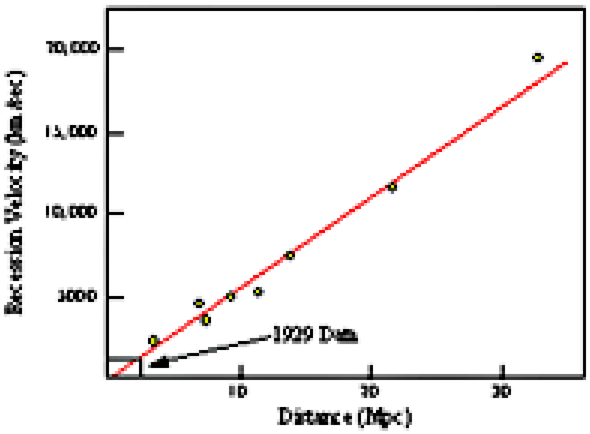

Freedman and Madore, "The Hubble Constant," Annu. Rev. Astron. Astrophys. , 2010, 48:673

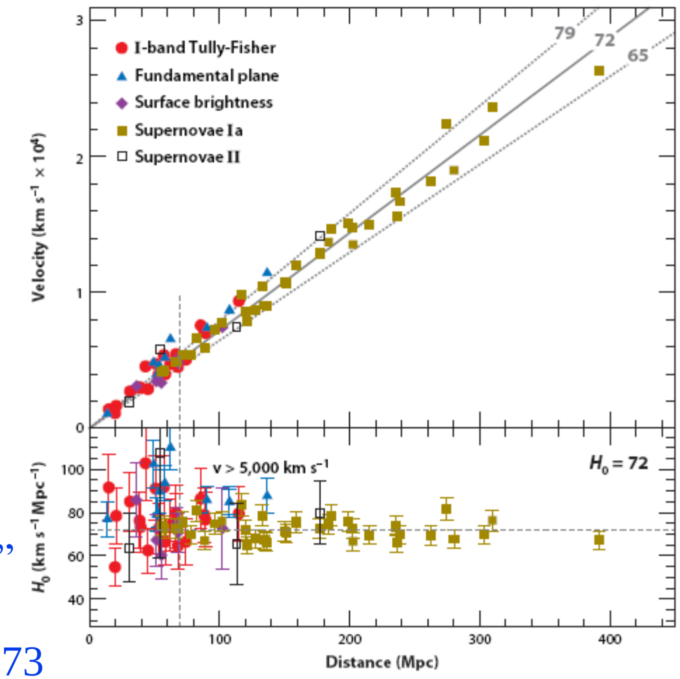

HST

CCD cameras for astronomy (cont')

One of the most distant galaxies ever observed, z ~ 7.3

Shibuya et al, Astrophysical Journal, 752, 11, 2012 and
Subaru telescope news release
http://www.naoj.org/Pressrelease/2012/06/03/index.html

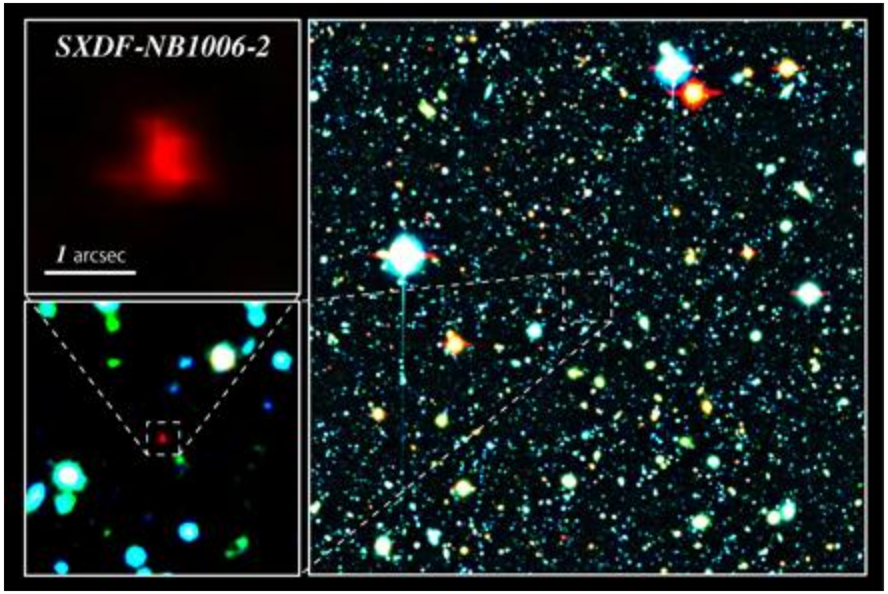

Color composite image of the Subaru XMM-Newton Deep Survey Field. Right panel: The red galaxy at the center of the image is the most distant galaxy, SXDF-NB1006-2. Left panels: Close-ups of the most distant galaxy. (Credit: NAOJ)

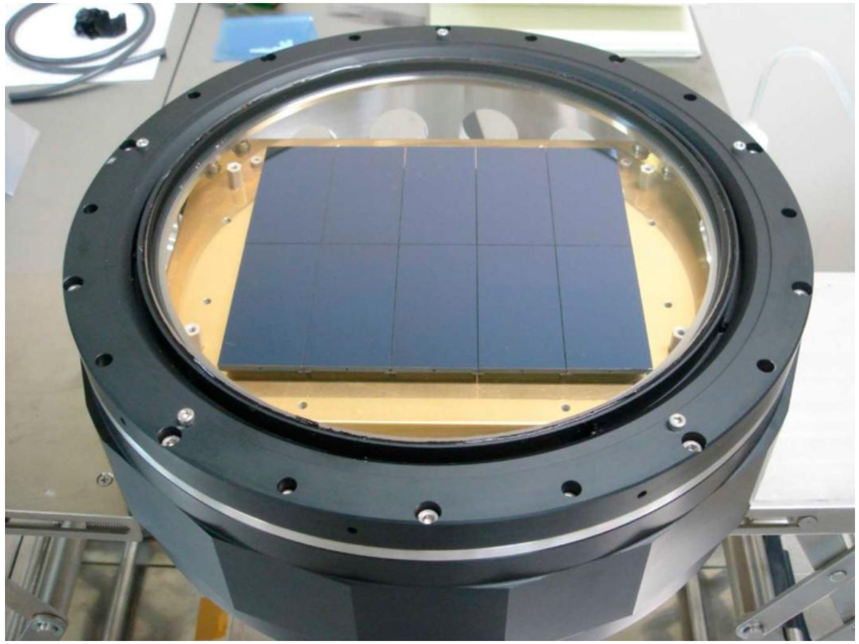

SuprimeCam – 10 2k x 4k, (15 μm)^2 pixel CCDs
Subaru 8-m Telescope (2008)

~ 200 μm thick, fully depleted CCDs
Fully depleted with substrate bias voltage
Hamamatsu Corporation

Importance of near-IR response

THE ASTROPHYSICAL JOURNAL, 752:114 (11pp), 2012 June 20 doi:10.1088/0004-637X/752/2/114

THE FIRST SYSTEMATIC SURVEY FOR Lyα EMITTERS AT $z = 7.3$ WITH RED-SENSITIVE SUBARU/SUPRIME-CAM*

TAKATOSHI SHIBUYA[1,2], NOBUNARI KASHIKAWA[1,2], KAZUAKI OTA[3], MASANORI IYE[1,2,4], MASAMI OUCHI[5,6], HISANORI FURUSAWA[2], KAZUHIRO SHIMASAKU[7,8], AND TAKASHI HATTORI[9]
[1] Department of Astronomical Science, The Graduate University for Advanced Studies, Mitaka, Tokyo 181-8588, Japan; takatoshi.shibuya_at_nao.ac.jp
[2] Optical and Infrared Astronomy Division, National Astronomical Observatory, Mitaka, Tokyo 181-8588, Japan
hirakawa-Oiwake-cho, Sakyo-ku, Kyoto 606-8502, Japan
ity of Tokyo, Mitaka, Tokyo 181-8588, Japan
iversity of Tokyo, Kashiwa 277-8582, Japan
AS, University of Tokyo, 5-1-5 Kashiwanoha, Kashiwa, Chiba 277-8583, Japan
ence, The University of Tokyo, Tokyo 113-0033, Japan
of Science, The University of Tokyo, Tokyo 113-0033, Japan
Vohoku Place, Hilo, HI 96720, USA
ted 2012 April 8; published 2012 June 4

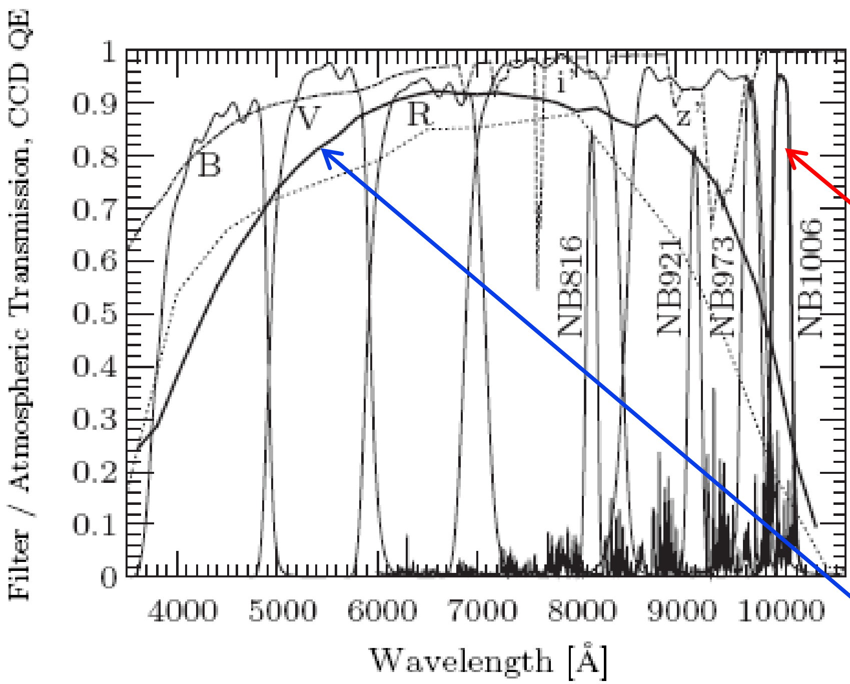

Figure 1. Filter transmission curves of the Suprime-Cam BB and NB filters and the new *NB1006* filter are shown with corresponding labels. The spiky profile at the bottom represents the OH airglow lines. The OH airglow lines are not strong, though not completely absent, at wavelength in the *NB1006* filter. The long dashed curve at the top shows the atmospheric transmission. The short dashed and thick solid curves show the quantum efficiency of the previous MIT/LL CCDs and the new fully depleted CCDs, respectively.

Searching for Lyman α line (Hydrogen) using narrow-band filter centered at 1.0052μm :

Emission wavelength 121.6 nm (UV)
Red-shifted to ~ 1.01 μm (near-IR)

Red shift ~ 7.3 (12.91 billion light years from Earth)
~ 14 hr exposure (30 minutes/exposure)

Subaru Suprime-CAM CCD quantum efficiency
200 μm thick fully depleted CCDs

Importance of near-IR response

The Dark Energy Survey Camera will have significantly improved detection ability for high red-shift supernova studies

Expect to detect ~ 4000 SN out to z ~ 1.2 and observe over 300 million galaxies

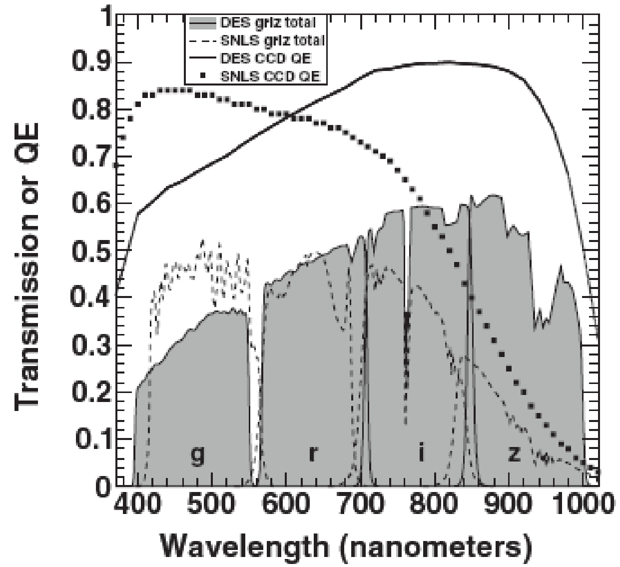

Figure 2. Comparison of the SNLS (Regnault et al. 2009) and DECam total transmission (H. Lin 2011, private communication) for an air mass of 1.3. Also shown is the CCD quantum efficiency (QE). The total transmission includes the effects of QE, the atmosphere, and the optical systems of the relevant cameras. Note the increased DES sensitivity at redder wavelengths. The DECam transmission is based on measurements of the full-size filters, which was not available during the simulations performed for this analysis. The assumed transmission in this paper is about 10% smaller than the measured values.

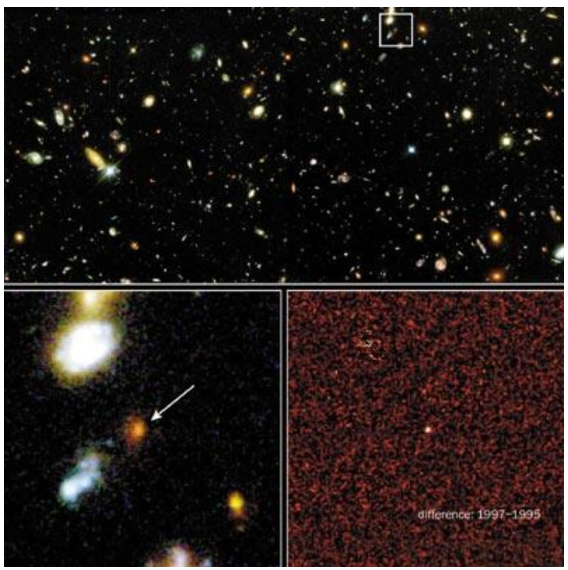

The Astrophysical Journal, 753:152 (25pp), 2012 July 10 doi:10.1088/0004-637X/753/2/152

SUPERNOVA SIMULATIONS AND STRATEGIES FOR THE DARK ENERGY SURVEY

J. P. Bernstein[1], R. Kessler[2,3], S. Kuhlmann[1], R. Biswas[1], E. Kovacs[1], G. Aldering[4], I. Crane[1,5], C. B. D'Andrea[6], D. A. Finley[7], J. A. Frieman[2,3,7], T. Hufford[1], M. J. Jarvis[8,9], A. G. Kim[4], J. Marriner[7], P. Mukherjee[10], R. C. Nichol[6], P. Nugent[4], D. Parkinson[10], R. R. R. Reis[7,13], M. Sako[11], H. Spinka[1], and M. Sullivan[12]
[1] Argonne National Laboratory, 9700 South Cass Avenue, Lemont, IL 60439, USA
[2] Kavli Institute for Cosmological Physics, The University of Chicago, 5640 South Ellis Avenue, Chicago, IL 60637, USA
[3] Department of Astronomy and Astrophysics, The University of Chicago, 5640 South Ellis Avenue, Chicago, IL 60637, USA
[4] E. O. Lawrence Berkeley National Laboratory, 1 Cyclotron Road, Berkeley, CA 94720, USA
[5] Department of Physics, University of Illinois at Urbana–Champaign, 1110 West Green Street, Urbana, IL 61801-3080, USA
[6] Institute of Cosmology and Gravitation, University of Portsmouth, Dennis Sciama Building, Burnaby Road, Portsmouth PO1 3FX, UK
[7] Center for Particle Astrophysics, Fermi National Accelerator Laboratory, P.O. Box 500, Batavia, IL 60510, USA
[8] Centre for Astrophysics, Science and Technology Research Institute, University of Hertfordshire, Hatfield, Herts AL10 9AB, UK
[9] Physics Department, University of the Western Cape, Cape Town 7535, South Africa
[10] Department of Physics and Astronomy, Pevensey 2 Building, University of Sussex, Falmer, Brighton BN1 9QH, UK
[11] Department of Physics and Astronomy, University of Pennsylvania, 203 South 33rd Street, Philadelphia, PA 19104, USA
[12] Department of Physics, Denys Wilkinson Building, Oxford University, Keble Road, Oxford OX1 3RH, UK

Received 2011 November 5; accepted 2012 May 7; published 2012 June 25

Near-IR spectroscopy (high-red shift quasar)

THE ASTROPHYSICAL JOURNAL, 736:57 (8pp), 2011 July 20 ZEIMANN ET AL.

Quasars:

Luminous cores of distant galaxies with supermassive black holes at their centers

Probe of early Universe

Hydrogen Lyman α line used to determine red-shift (121.6 nm, UV)

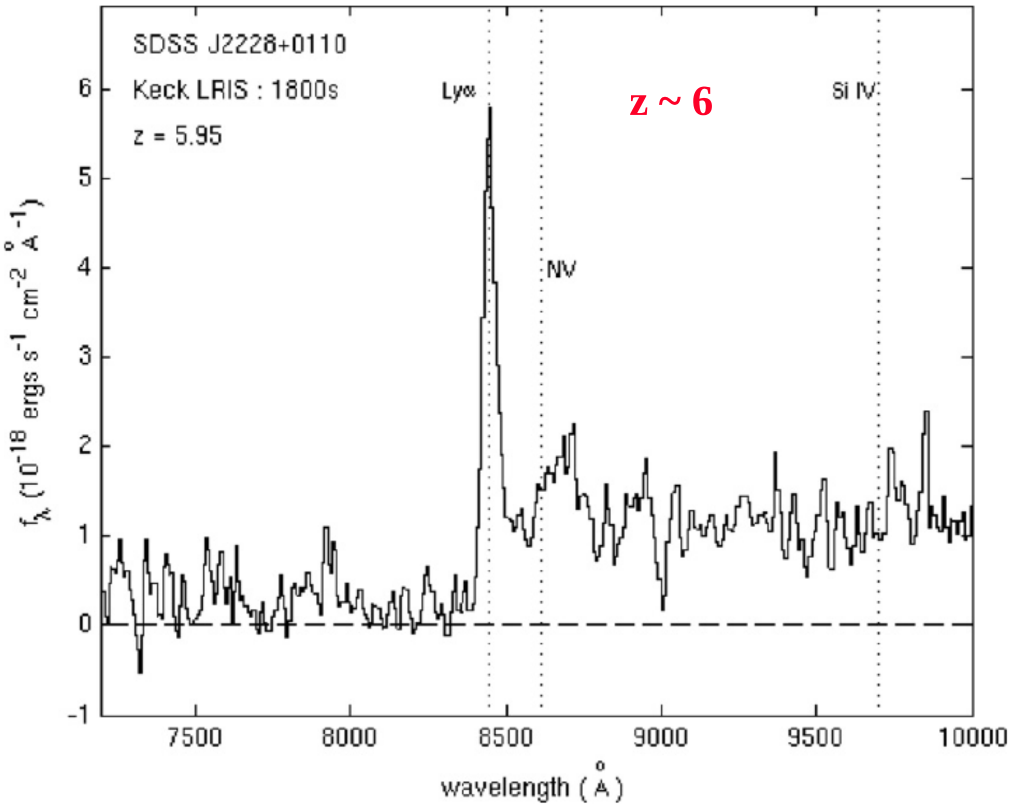

Figure 4. Spectrum of SDSS J222843.54+011032.2 obtained in 2010 June using LRIS on the Keck 1 telescope. The spectrum has been binned using inverse sky-variance weighting to reduce the sky noise. Only the two best out of the total four exposures were used to make this optimal spectrum. The redshift, $z = 5.95$, was calculated using the peak of the identified Lyα emission line. The expected locations of other typical emission lines are labeled with a vertical dotted line.

Keck 10-m Low Resolution Imaging Spectrograph
Two 2048 x 4096, (15 μm)^2-pixel CCDS (DALSA/LBNL)

BOSS

- Baryon Oscillation Spectroscopic Survey (SDSS-III)
  - —5 year goal is to measure spectra and red-shift of 1.5 million galaxies (z ~ 0.4 – 0.7) and 160k quasars (z ~ 2.2 – 3)
  - —Fiber-fed, multi-object spectroscopy (1000 at a time)
    - Aluminum plates with precise holes to match galaxies
  - —Precision measurement of galaxy clustering due to sound waves in the early universe (cosmic ruler ~ 500 light years)

David Schlegel, BOSS PI

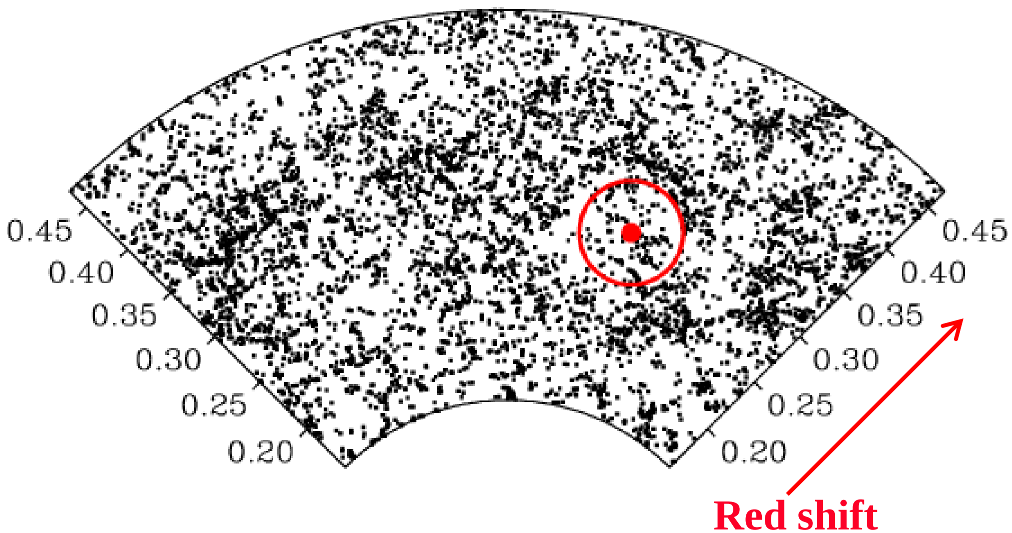

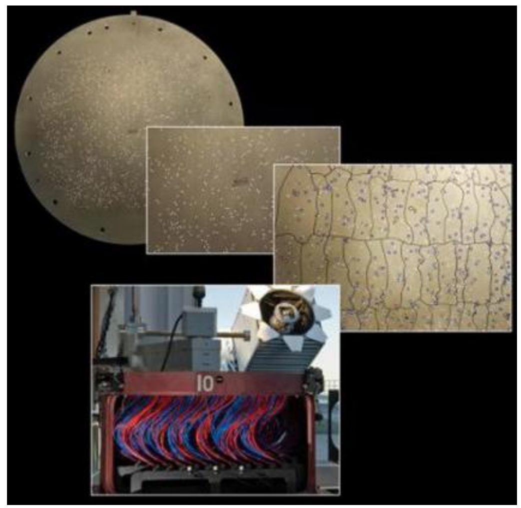

Galaxy spectrum from BOSS DR9 data release DR9

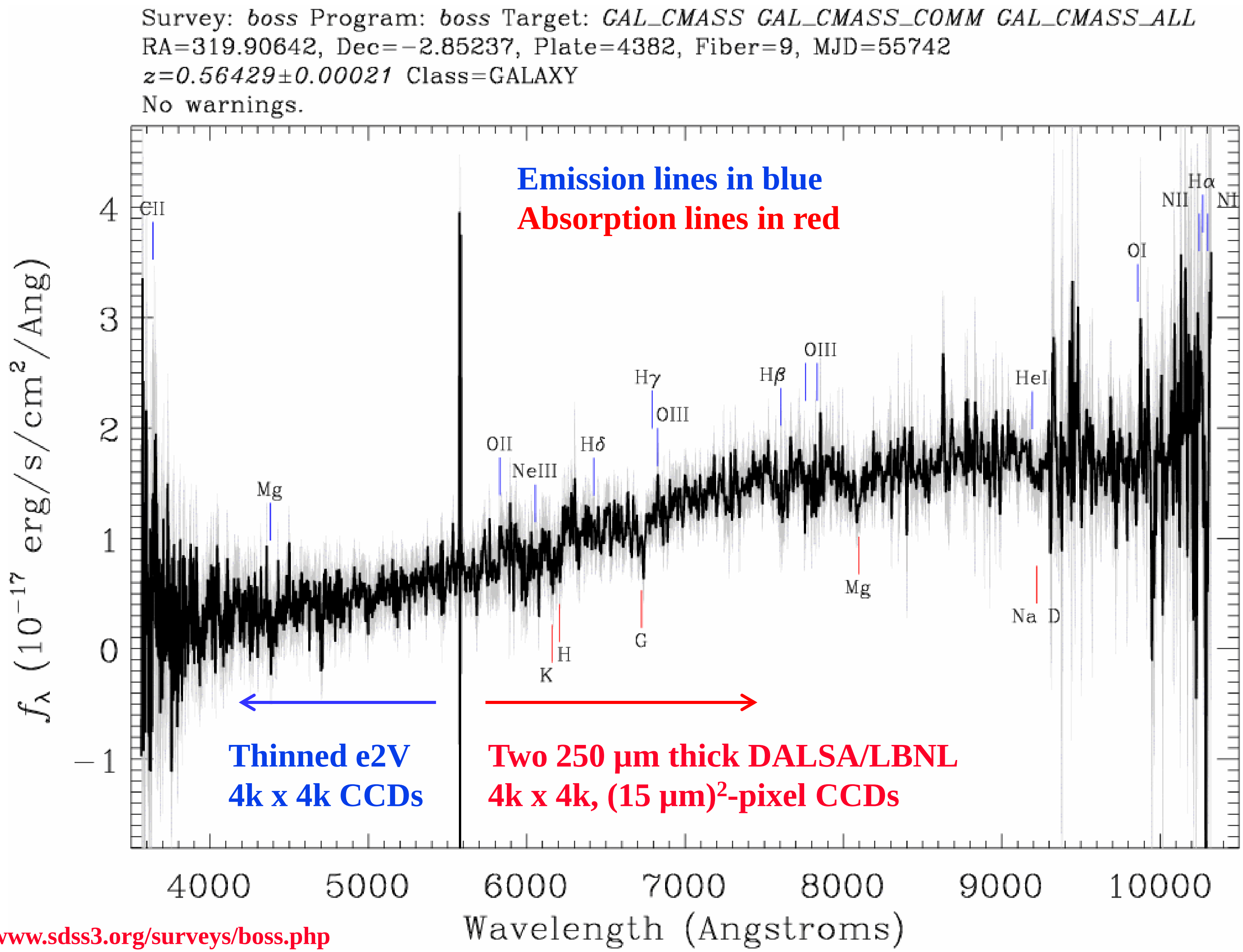

http://www.sdss3.org/surveys/boss.php

BOSS

- Two 4k x 4k LBNL CCDs in red spectrograph (mid 2009)
- 6 cm x 6 cm imaging area – needed for BOSS throughput

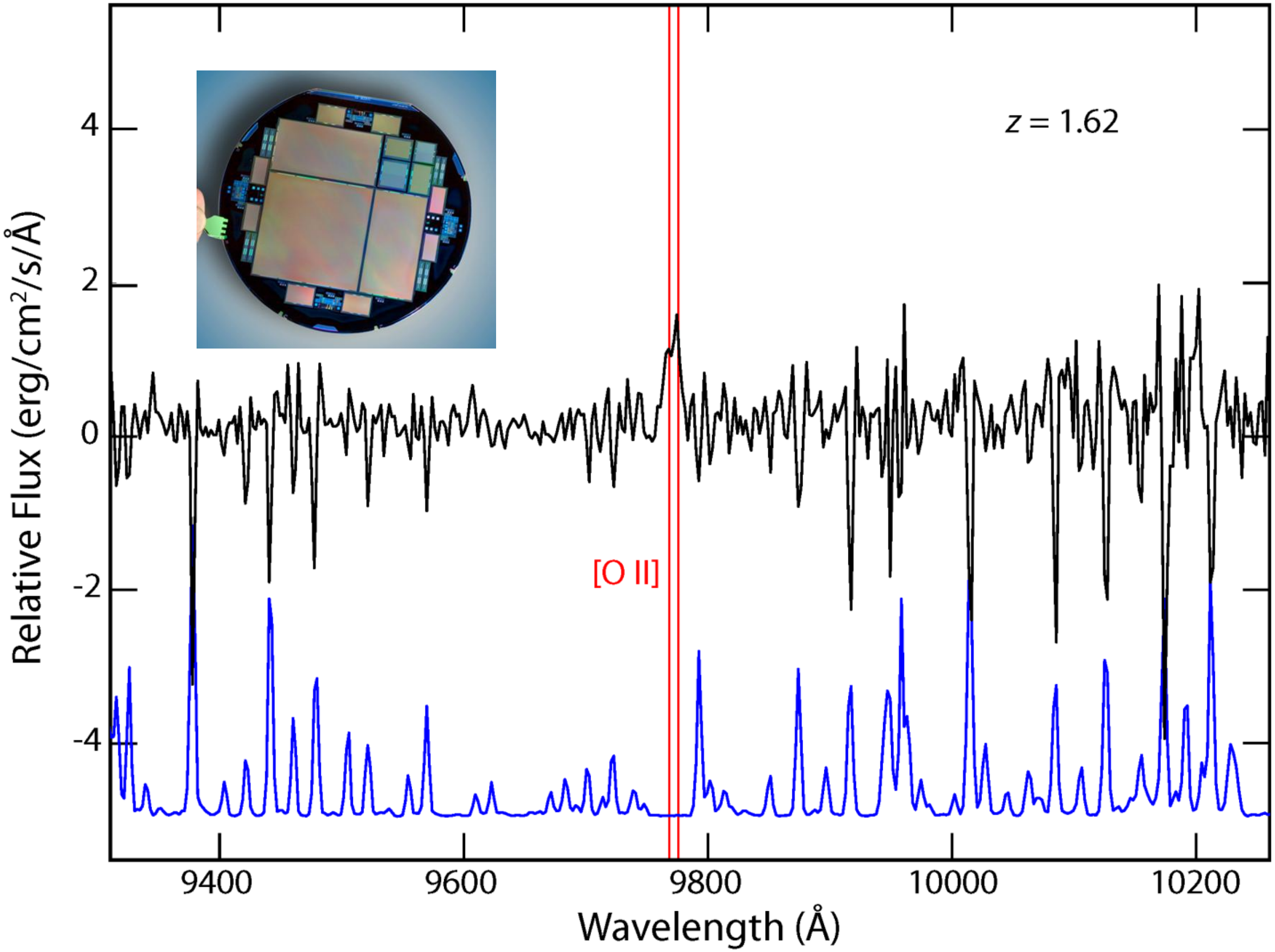

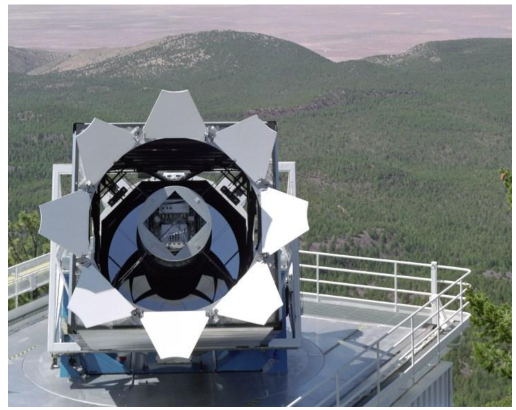

Spectra courtesy of SDSS-III project

Sky background in blue

1st scientific papers
260k galaxies
Spring 2012

Outline

- Fundamentals of CCDs and CMOS image sensors
- Scientific CCDs for astronomy
- Fully depleted CCDs fabricated on high-resistivity silicon – device physics/applications/**technology**
  - —**Important contributions from the Microlab**

LBNL fully depleted CCD development

1st high-ρ CCDs fabricated at LBNL

200 x 200, (15 μm)^2 pixel, 300 μm thick, fully depleted CCDs on 100 mm diameter, ~ 10,000 Ω-cm silicon

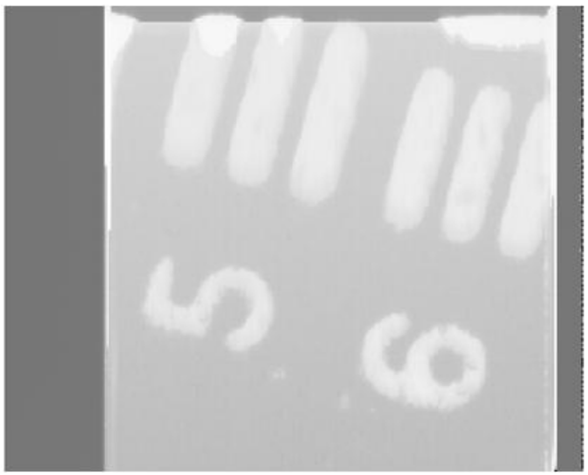

1st image, Lick Observatory CCD Lab
May 1996

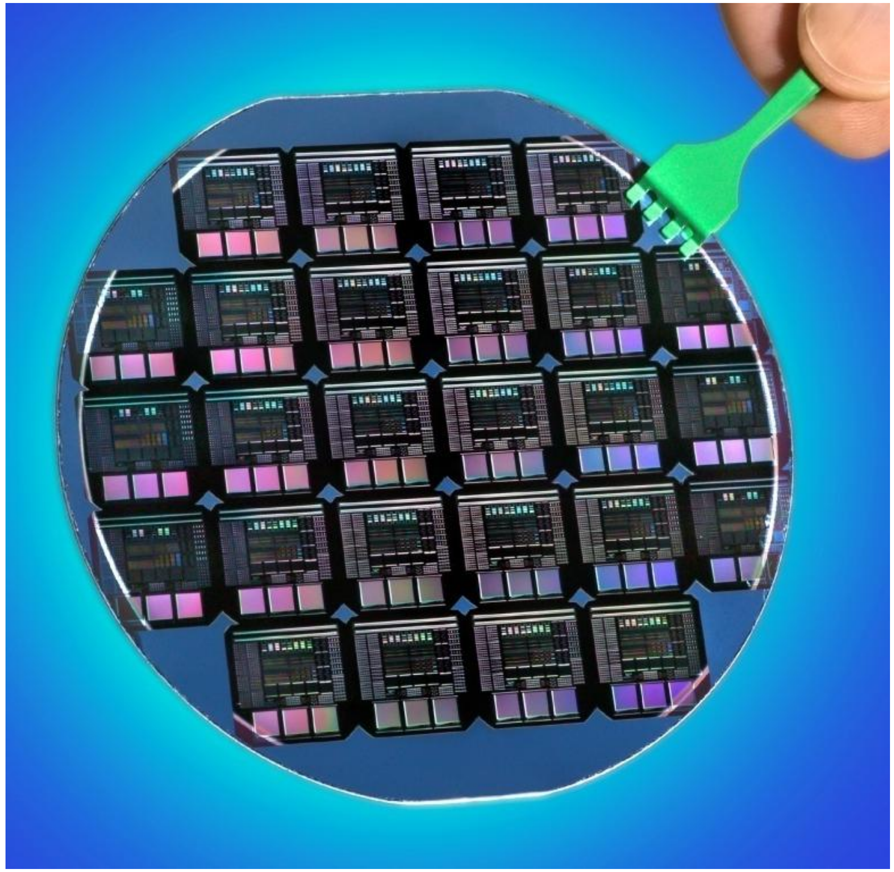

100 mm diameter, high-resistivity Si wafer

LBNL fully depleted CCD development

Initially all fabrication steps were done in the LBNL MicroSystems Laboratory Class 10 cleanroom except

- Ion implantation (Bay Area vendors)
- Polysilicon etching (UC-Berkeley Microlab Lam4)
  Critical step given the need for substantial overetch with high selectivity to gate nitride layer

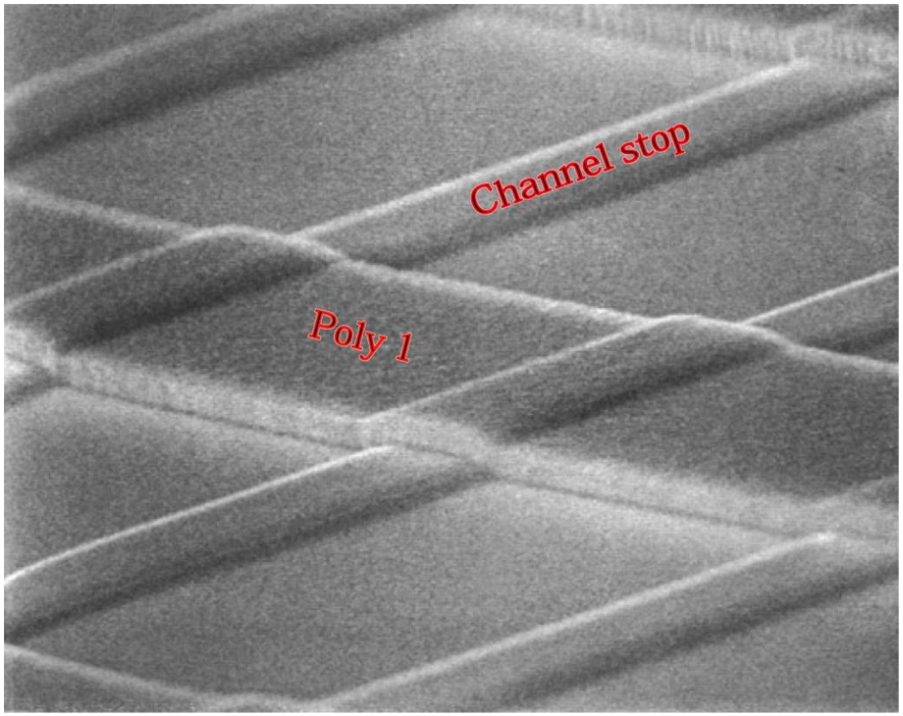

LBNL fully depleted CCD development

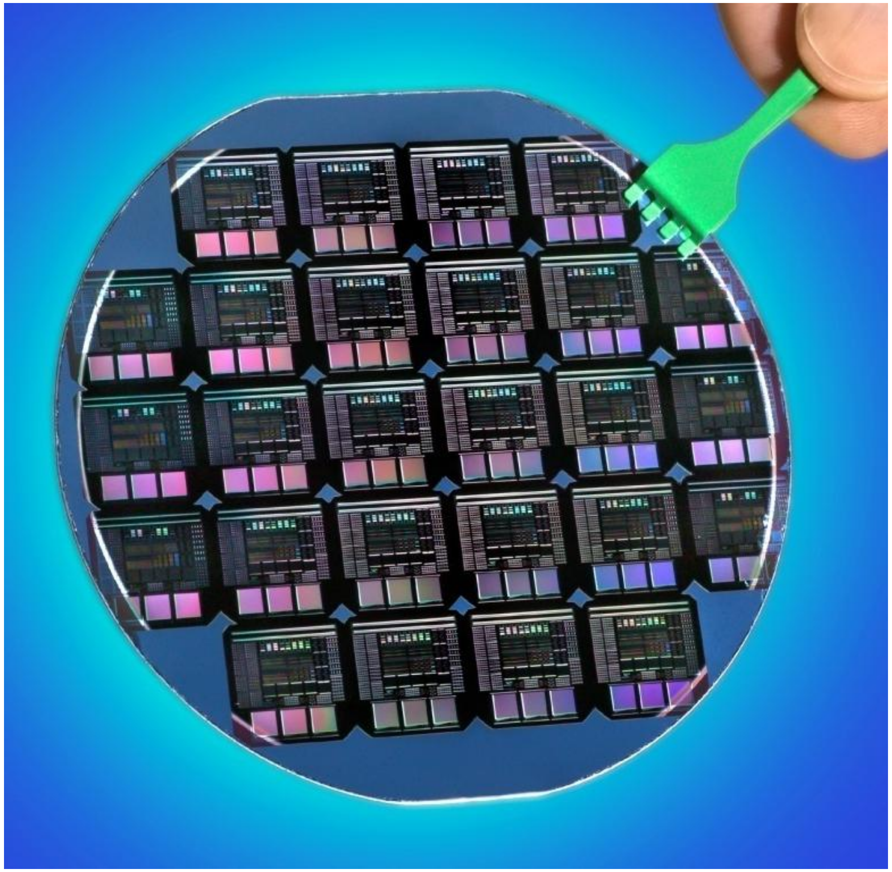

100 mm diameter, high-resistivity Si wafer

The exposure area of the GCA step and repeat lithography tool was too small for the large format CCDs required for astronomy and astrophysics

LBNL fully depleted CCD development

Donation of Perkin Elmer Micralign from Intel to LBNL via UC-Berkeley Microlab facilitated by Bob Hamilton allows for large format CCDs to be produced by 1x projection lithography

2k x 2k
15 µm

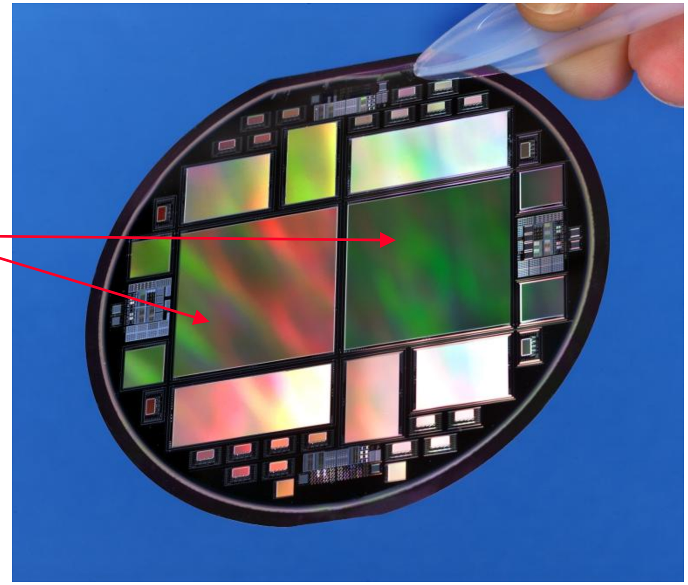

100 mm
wafers

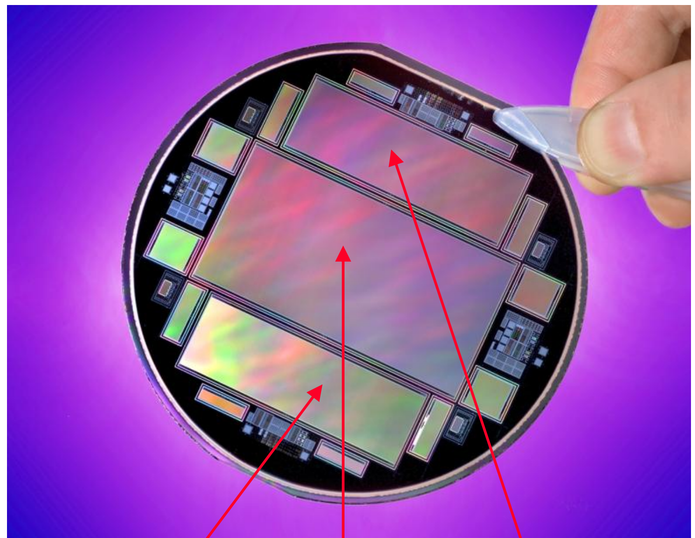

1478 x 4784 10.5 µm	2k x 4k 15 µm	1294 x 4186 12 µm

Present-day process flow

- Majority of CCD processing at Teledyne DALSA
  - —8 of the 11 photomasking steps done at DALSA
  - —Take advantage of foundry efficiency, high yield

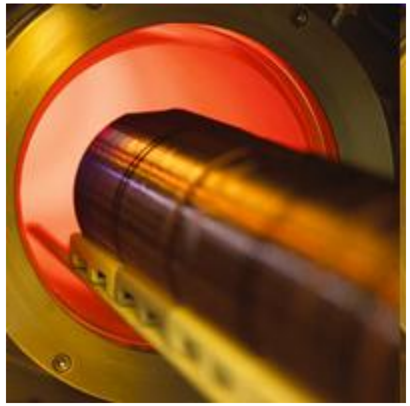

2.5 µm CCD technology with scanner lithography for large-area CCD fabrication

150 mm diameter wafers

Present-day process flow

- 3 wafers completed at DALSA for Q/C, 21 to LBNL
  - —Thinned at commercial vendors (backgrind/CMP)
    - 200 - 250 µm typically, recent work at 500 µm
  - —Processed to completion at LBNL

MicroSystems Laboratory
Class 10 clean room

Present-day process flow

- LBNL processing
  - —Thin backside contact (in-situ doped polysilicon)
  - —Contact/metal mask
  - —Backside anti-reflection coatings

MicroSystems Laboratory
Class 10 clean room

Present-day process flow

- LBNL processing
  - —Key point – Back illuminated processing at the wafer level and in batch mode

MicroSystems Laboratory
Class 10 clean room

DES camera – CCD fabrication summary

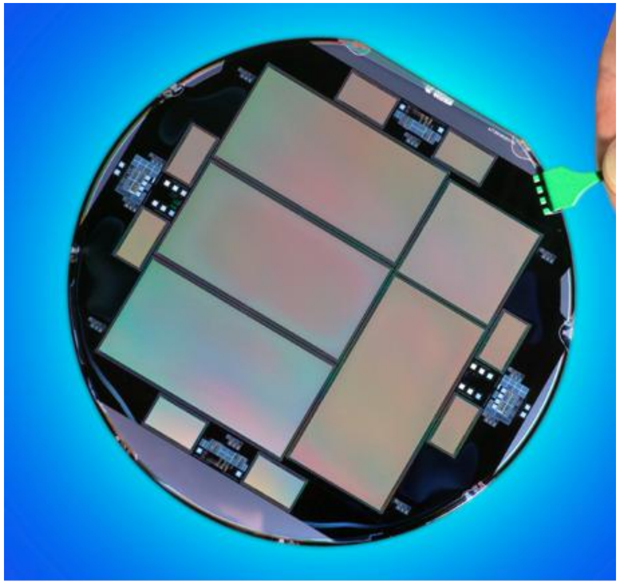

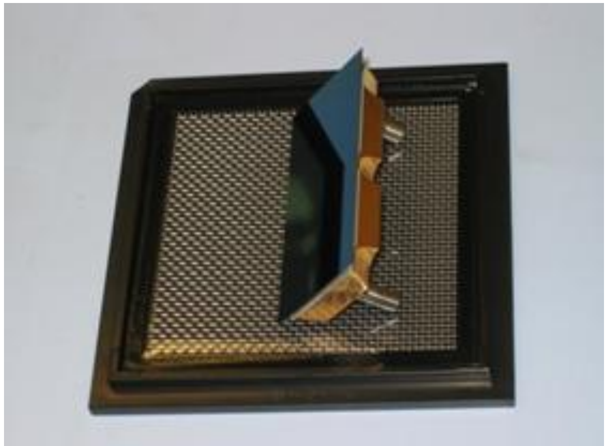

2k x 4k CCD in FermiLab
4-side buttable package
Image courtesy of T. Diehl (FNAL)

- 7 lots fabricated at DALSA/LBNL (21 wafers/lot)
- 124 science-grade CCDs produced
  - Overall yield for the 7 lots was ~ 21%
- Yield improvements resulted in 58 science-grade CCDs produced from the final 2 production lots
  - ~ 35% yield final 2 production lots
- CCDs selected for the camera had on average less than one bad column per CCD
  - Percent bad pixels 0.014%

Packaging and final testing at FNAL
CCD flatness better than 10 μm
Focal plane better than 60 μm

Current LBNL CCD efforts on 150 mm diameter wafers with DALSA Semiconductor

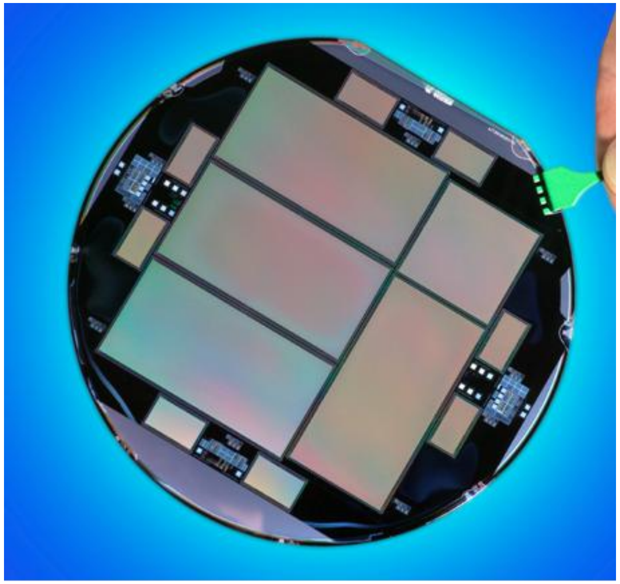

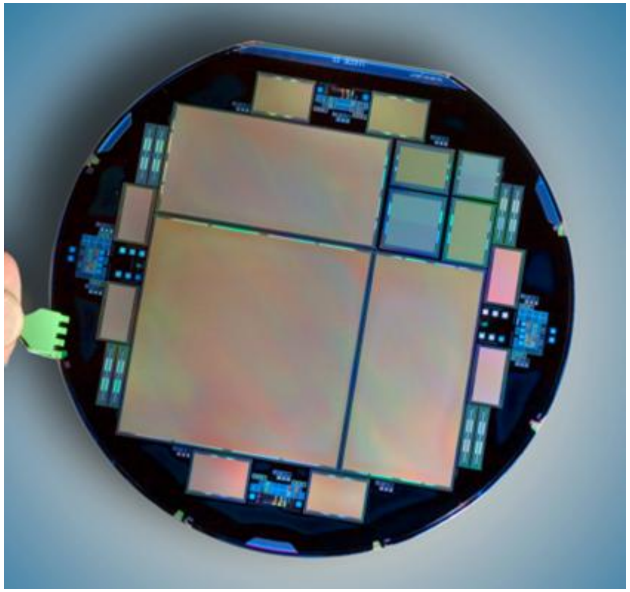

Dark Energy Survey camera wafer (FNAL)

124 2k x 4k CCDs produced for DECam

Keck LRIS

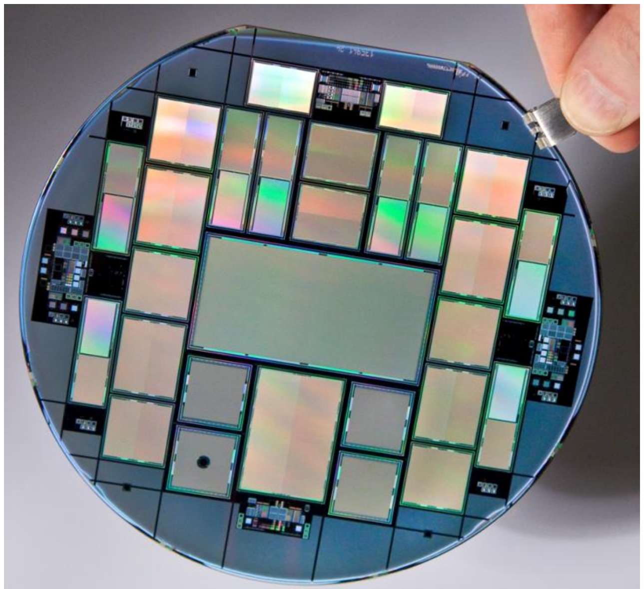

4k x 4k wafer

BOSS spectrograph since 2009 and NOAO KOSMOS/COSMOS instruments (coming soon)

R&D wafer (lower noise, faster readout, direct detection of x-rays)

Current LBNL CCD efforts on 150 mm diameter wafers with DALSA Semiconductor

- LBNL Engineering Group – 200 fps CCDs for direct detection of low-energy x-rays

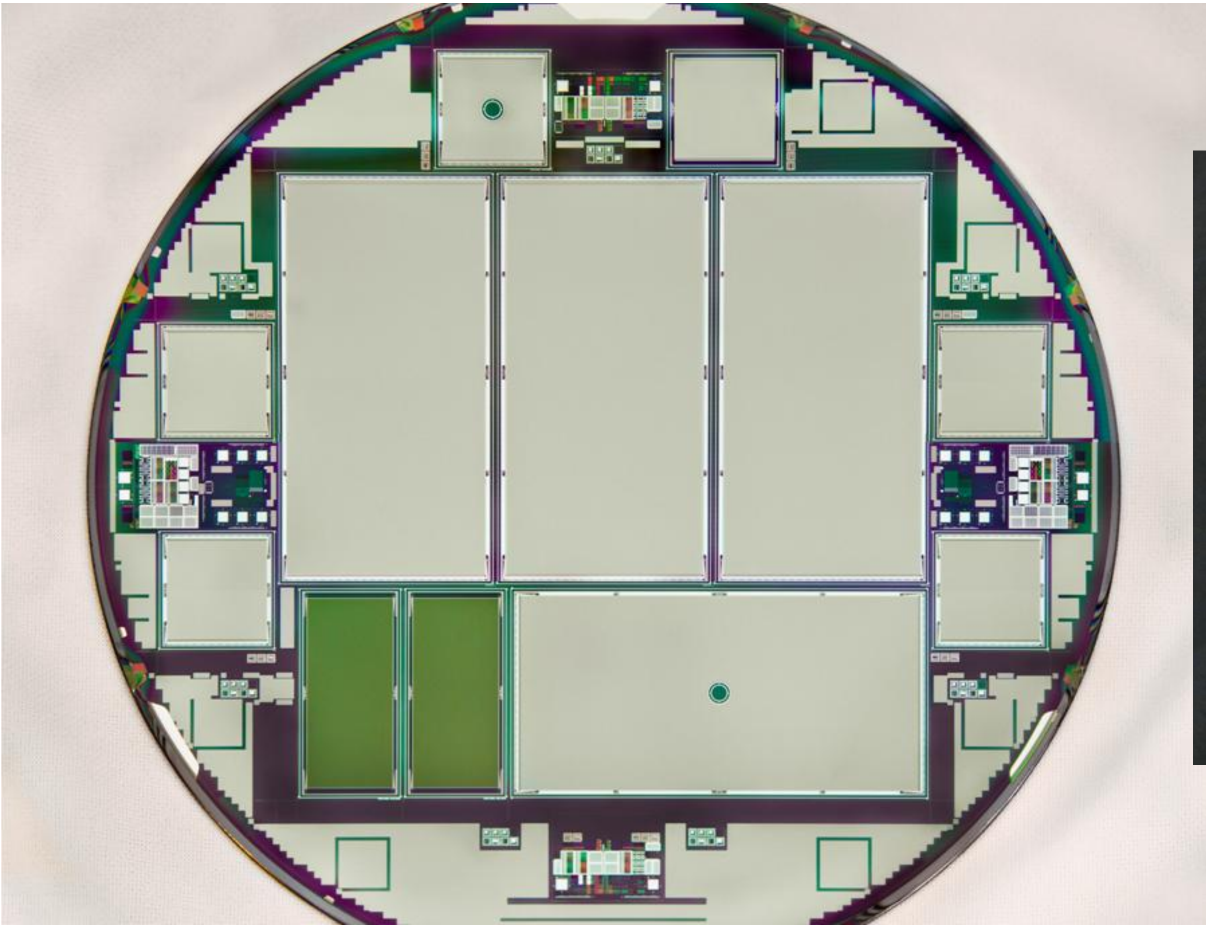

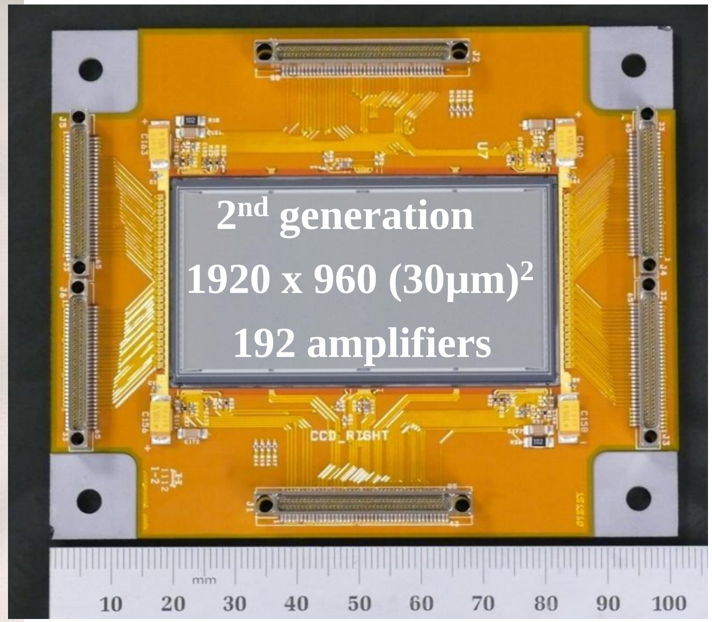

Amplifiers every 10 columns, metal strapping of poly, and custom IC readout

Acknowledgements – LBNL CCD staff

MSL

Co Tran, Guobin Wang, Nick Palaio, Steve Holland

Testing

Armin Karcher, Sufia Haque, Bill Kolbe, Julie Lee

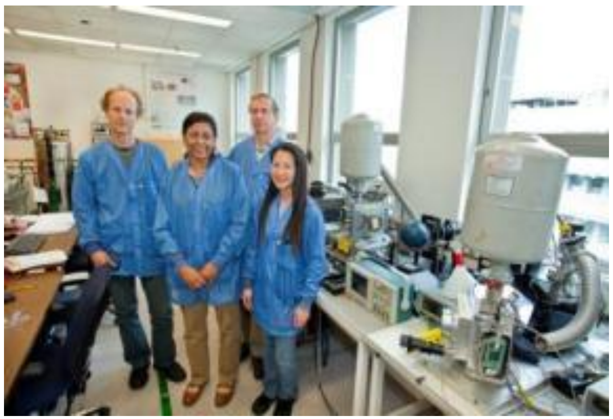

Probing / Packaging

John Emes

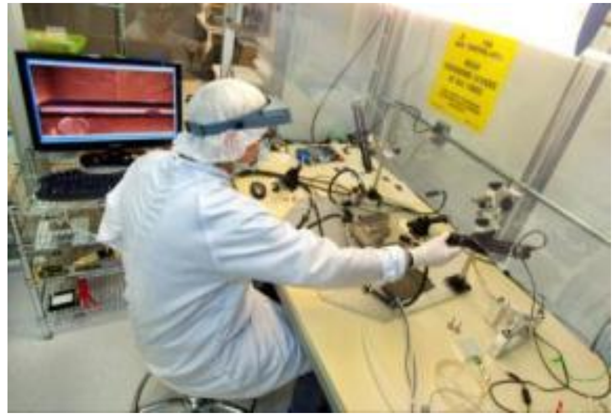

Plus Chris Bebek (group leader), Natalie Roe (former group leader), and Don Groom

Thank you for your attention